

Chapter 3

Constructing synthetic gene networks to control decision-making in the yeast mating pathway

Abstract

Cells utilize internal molecular networks to direct cell fate via the integration and processing of extracellular information. Control of these decision-making pathways offers the potential to intervene in aberrantly activated programs as well as direct complex, multicellular tasks such as tissue development. Programming of diverse cellular behaviors may be accomplished by the development of synthetic circuits capable of activating and attenuating the response from internal signaling pathways. Previously constructed positive and negative molecular network diverters encoding a single pathway regulator demonstrated small-molecule-dependent routing to divergent alternative fates. However, simultaneous integration of these previously demonstrated positive and negative diverters results in diverter antagonism and fails to allow dual-routing to both alternative fates. In this work, we demonstrate the construction of more complex diverter networks with integrated positive and negative routing functions that allow the conditional induction of alternative cell fates based on small-molecule input. By constructing networks with two differentially regulated expression modules composed of stringent RNA-based controllers we were able to limit diverter antagonism, amplify pathway activation, and induce pathway attenuation allowing genetically identical cells to be conditionally routed to one of three fates in response to environmental cues. In constructing these networks we identified sensitive parameters for balancing and tuning diverter function and demonstrate the rational tuning of both diverters to allow dual-fate routing. Further, we demonstrate the construction of networks that suppress subthreshold noise in gene expression to robustly amplify differences in environmental input and achieve enhanced resolution between triggered and non-triggered cell populations.

Expanding synthetic control to mammalian systems via the elucidated molecular network diverter strategies and principles will facilitate the construction of sophisticated synthetic programs to achieve higher-order cellular functions such as the patterning of cell fate, tissue homeostasis, and autonomous immune surveillance.

Introduction

Biological systems process environmental signals via native regulatory networks directing complex processes such as development, tissue homeostasis, and the immune system response [1]. The temporal and spatial distribution of molecular signals enables responses to be coordinated in time and space via the distributed processing of these signals by individual cells, resulting in orchestrated system responses such as organogenesis, wound healing, and pathogen elimination [2-4]. Synthetic circuits that can interface with and redirect these processes offer the potential to orthogonally regulate complex cellular behaviors. However, construction of an interface that provides for specific pathway information to be translated via synthetic circuitry into changes in the native network still poses a major challenge in synthetically regulating cell fate [5, 6]. Further, synthetic circuits that can be tuned via their component parts as well as architecture will facilitate expansion of such circuits to native networks with a range of associated properties [7]. The development of parts that allow orthogonal tuning of system performance without modification of other potentially constrained regulatory elements (e.g., promoters, genes) will enable greater flexibility in adapting synthetic circuits to be regulators of cellular behavior.

In previous work, a type of synthetic gene circuit, referred to as a molecular network diverter, was applied to controlling signaling and fate decisions in a model MAPK pathway in response to distinct environmental triggers. Specifically, we constructed positive and negative diverters that were used to turn the activity of the *Saccharomyces cerevisiae* mating pathway on and off, respectively. The positive network diverter activated the pathway in the absence of the canonical pathway input, thereby

routing cells to the alternative “promiscuous” fate. The negative network diverter inactivated the pathway even in the presence of the canonical pathway input (pheromone), routing cells to the “chaste” fate. The positive and negative diverters are programmed to respond to distinct small-molecule inputs, allowing independent channels by which to activate each diverter. Thus, we propose integrating positive and negative diverters within the same cell to achieve conditional routing of cells to three distinct cell fates. In the absence of either environmental trigger, cells will adopt the wild-type fate as the diverters run quiescently. However, when called by their respective triggers, each diverter is intended to route cells to the programmed alternative fates: chaste or promiscuous.

Molecular network diverters are composed from expression modules containing three genetic parts; a promoter, a pathway regulator, and a RNA-based controller (Figure 3.1). The properties of these parts dictate the function and performance of the diverter. The sign of the diverters, positive or negative, is determined by whether the pathway regulator activates or attenuates pathway activity in the network, respectively. The promoter determines the mode of expression, feedback or nonfeedback, as well as the strength of the diverter activity. RNA controllers provide a second layer of control by which to tune diverter activity and allow the molecular network diverter to respond to environmental signals. Small-molecule-responsive RNA-based controllers, also called RNA switches, are an engineered class of non-coding RNA that allows for conditional control from any promoter-gene pair via a chemical trigger [8]. Choice of the switch specifies the small-molecule trigger that activates the diverter and tunes the diverter activity. Combining these three parts together in various configurations generates a

variety of expression modules. Dependent on the context of implementation, these expression modules can perform independently as molecular network diverters or be integrated into larger networks of synthetic circuitry. Previous work has shown that single-module diverters, composed of one expression module, can be implemented to conditionally route cells to an alternative fate. However, to access both alternative fates the simultaneous integration of positive and negative diverters is required.

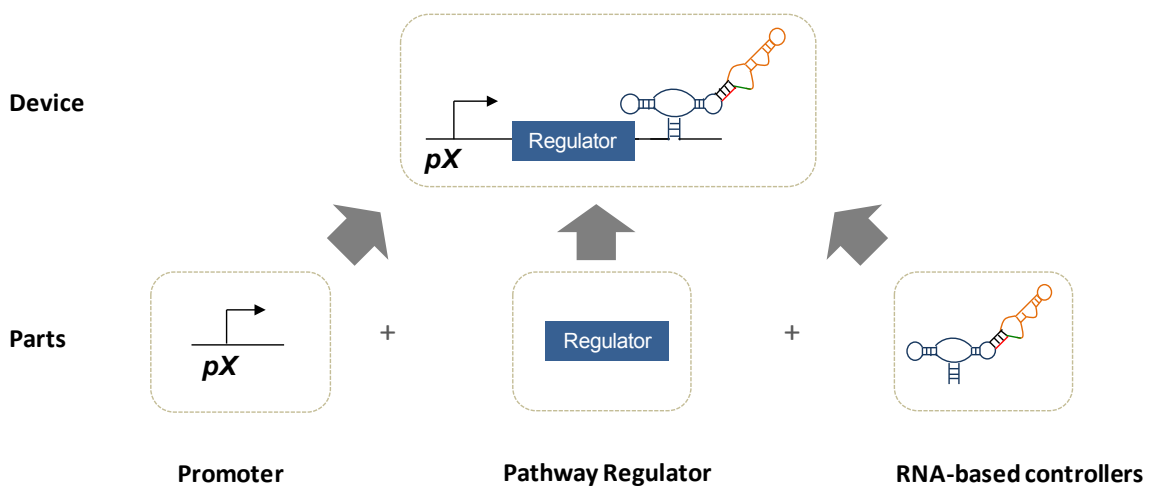


Figure 3.1. Composition of an expression module from well-defined parts. Molecular network diverters contain various expression modules which are composed of a promoter, a pathway regulator, and a RNA-based controller, also called a switch. The promoter specifies the expression mode (e.g., constitutive or feedback) which determines the network connectivity. The promoter and switches combine to determine the expression strength and thus the activity of the diverter. Additionally, switches specify which small-molecule input regulates expression and the range of expression across ligand concentrations. The pathway regulator's interaction with the native molecular network determines the pathway response curve. The pathway response curve can be altered by changes in network connectivity due to feedback expression of regulators.

One potential challenge that may be encountered in integrating network diverters encoding opposing functions is antagonization, or competition between the opposing activities encoded in the diverters. Antagonization may hinder the diverter's ability to route cells to both alternative fates. Specifically, the positive and negative diverters measurably change the basal activity of the pathway in the absence of their respective triggers. While these sub-threshold changes in activity are insufficient to route cells to an

alternative fate, they may antagonize the activity and routing capability of an opposing diverter. Issues with basal expression levels from synthetic regulatory networks impinging on circuit performance have been previously reported [9-11]. One strategy used to increase the stringency associated with a synthetic network is to incorporate additional layers of post-transcriptional control via noncoding RNA control elements [5, 12, 13]. While strategies for reducing basal expression may also reduce triggered expression levels, modification of the regulatory network architecture through the incorporation of feedback loops may supplement the reduction in triggered expression levels via the amplification of the pathway response to the trigger.

Natural biological systems utilize feedback architectures to ensure proper function of diverse cellular processes. For example, positive and negative feedback loops are used to facilitate robustness in developmental processes by introducing ultrasensitivity and by maintaining homeostasis, respectively, [14-16]. More complex control architectures, such as coherent and incoherent feedforward loops, have been shown to function as persistence detectors, pulse generators, and response accelerators in natural and synthetic systems [17-19]. The proper configuration of such regulatory architectures within developmental pathways is posited to contribute to the robustness of multicellular organization critical for higher eukaryotes [14, 20-22]. For example, modeling of cell fate determination in flowers has predicted that network architecture in these systems constrains pathway activity to a few stable states independent of the chosen initial conditions or model parameters [23]. In addition, synthetic circuits that reshape natural molecular pathways have shown that cell fate can be routed by altering the native network topology [24]. Thus, network topology itself can ensure robust adoption of particular cell fates.

In this chapter, we show that simultaneously integrating positive and negative diverters in the yeast mating pathway, optimized for individual routing functions, fails to achieve routing to both alternative fates. In particular, routing to the promiscuous fate is hampered across the range of activities exhibited by the positive feedback diverters when paired with any negative diverter. Resistance introduced by basal level expression of *Msg5* from the negative (resistance) diverter may prevent pathway activation above the requisite threshold to trigger positive feedback-induced amplification. The addition of a positive expression (booster) module to the positive feedback diverter effectively counteracts this network antagonism to construct the amplifying diverter (Figure 3.2). The amplifying diverter allows promiscuous routing in the presence of the resistance diverter. However, the resistance diverter is unable to route cells to the chaste fate when implemented with the amplifying diverter. The data indicate that at high levels of pheromone, conditions in which positive feedback is amplified, the amplifying diverter overwhelms pathway inhibition by the resistance module. The addition of a negative feedback module to the resistance diverter results in an attenuating diverter that effectively balanced pathway response. Utilizing this double-module strategy, we successfully integrated the amplifying and attenuating diverters to achieve dual-fate routing to both alternative programmed cell fates. Our work shows that the performance of the amplifying and the attenuating diverters is highly sensitive to the strengths of the positive feedback and resistance modules. Further, our findings have important implications for the construction of networks that suppress noise amplification, amplify differences in environmental stimuli, and trigger robust cellular phenotypic programs in the face of antagonistic signals.

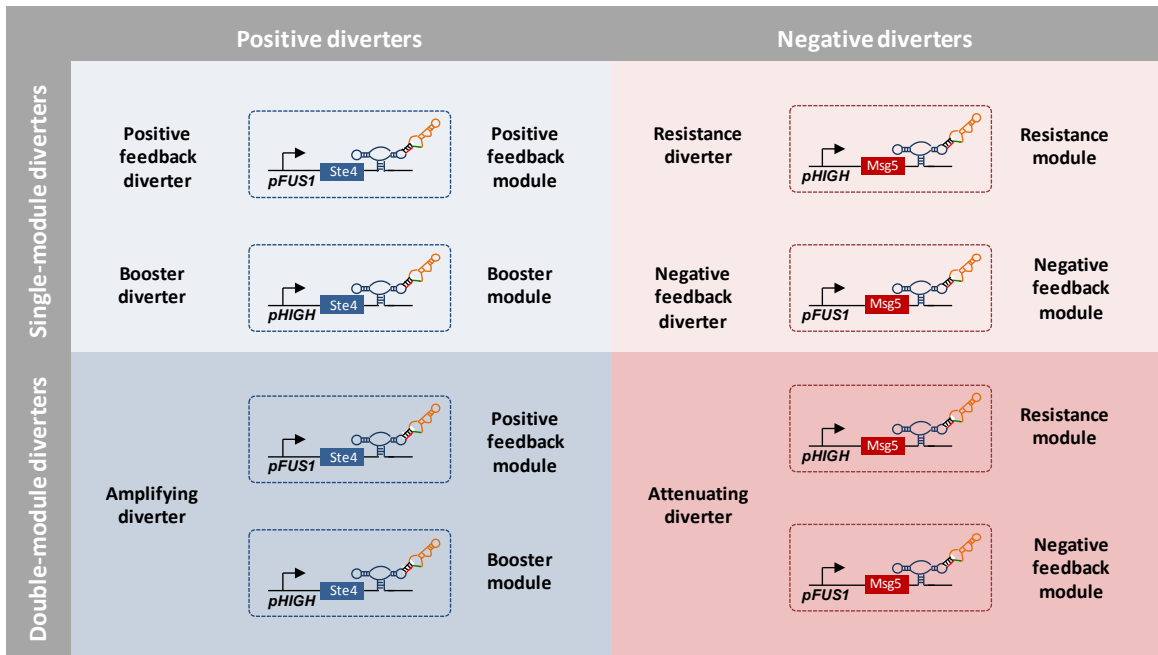


Figure 3.2. Molecular network diverters are composed from single- and double-expression modules that allow fate-routing dependent on small-molecule input. Six different types of diverters were constructed. The positive feedback diverter, the booster diverter, and the amplifying diverter represent the three types of positive diverters. The resistance diverter, the negative feedback diverter, and the attenuating diverter represent the three types of negative diverters. Diverter performance is determined by the composition of their expression modules. Four of the diverter types are single-module diverters containing only one expression module. The amplifying and the attenuating diverters are double-module diverters. The attenuating diverter is constructed with a positive feedback module and booster module. The attenuating diverter contains a resistance module and a negative feedback module.

Results

Simultaneous expression of single-module positive and negative diverters fails to route cells to either fate

The original molecular network diverters were optimized to independently route fate decisions in the yeast mating pathway and exhibited different regulatory architectures. The positive diverter integrated a positive network regulator (Ste4) with a feedback promoter (pFUS1) and a tetracycline-responsive RNA switch to compose the positive feedback diverter which activates pheromone-independent signaling through the

pathway in the presence the tetracycline, resulting in the so-called promiscuous fate. The negative diverter integrated a negative network regulator (Msg5) with a constitutive promoter (pHIGH) and a theophylline-responsive RNA switch constructing the resistance diverter to inhibit signaling through the pathway in the presence of theophylline even in the presence of pheromone, resulting in the so-called chaste fate.

We examined an initial dual diverter architecture based on integrating the positive and negative diverters optimized for independent cell fate routing. To examine optimal pairing of diverters encoding antagonistic functions, we paired the positive feedback diverter (pFUS1-Ste4-S3tc) with diverse resistance diverters incorporating a set of RNA switches exhibiting a range of activities (pHIGH-Msg5-Sx) (Supplementary Figure 3.1). Pathway activity was determined by measuring GFP expression levels from a transcriptional fusion construct (*pFUS1*-GFP, GFP fused to a mating responsive promoter). Fate routing was determined by observing mating-associated cell cycle arrest via halo assays (Materials and Methods). Cells adopting the chaste fate exhibit reduced halo formation as cells resist pheromone-induced cell cycle arrest. Cells adopting the promiscuous fate demonstrate persistent, pheromone-independent cell-cycle arrest outside the canonical halo region as indicated by reduced cell growth across the entire plate. The results indicate that within the dual diverter architecture the two diverters antagonize one another, diminishing diverter performance and leading to less robust fate switching (Figure 3.3). While several dual diverter configurations preserve weak routing to the chaste fate, promiscuous routing was not observed from any of the dual diverter configurations. In addition, pathway activation was not improved by increasing the strength of the positive feedback module (Supplementary Figure 3.2). The data indicate

that switching to the promiscuous fate may be hindered by basal expression levels of *Msg5* from the resistance module. Resistance may inhibit superthreshold pathway activation, which is necessary for amplification via the positive feedback loop, resulting in low pathway activation for a significant fraction of cells even in the presence of the positive molecular trigger (tetracycline).

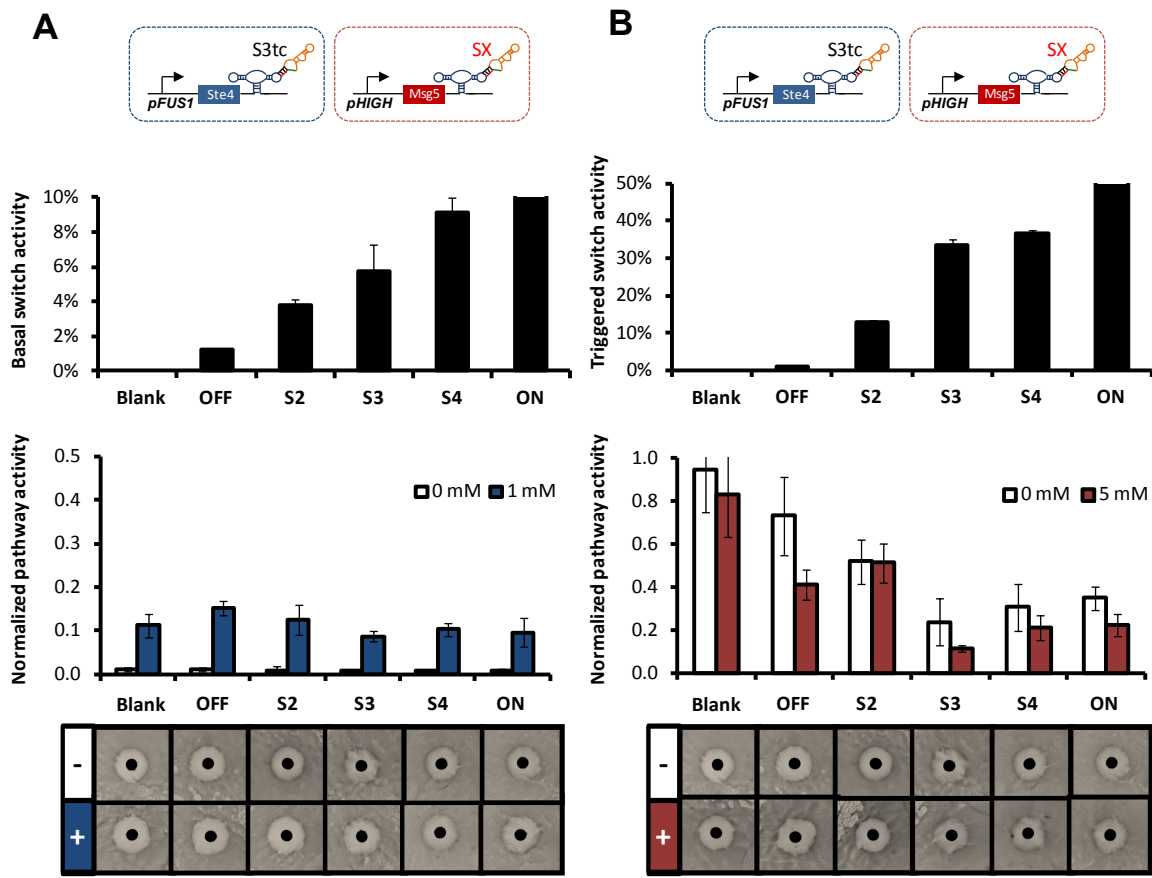


Figure 3.3. Integration of positive and negative single-module diverters fails to achieve dual-fate routing. **A.** A single-module positive feedback diverter, pFUS1-Ste4-S3tc, fails to route to the promiscuous fate in the presence of resistance diverters incorporating a range of switch strengths. The Blank control bears a plasmid without either diverter. Increasing positive feedback strength does not improve pathway activation from the positive diverter (Supplementary Figure 3.1). **B.** Negative diverters incorporating constitutive expression from pHIGH of *Msg5* and switches of varying strength show significant reduction of pathway activity, but weak routing to the chaste fate in halo assays.

Building network architectures to amplify trigger-induced switching to activate the mating pathway in the presence of antagonistic signals

We explored alternate architectures for the positive diverter to support increased pathway activation. A number of strategies can be implemented for increasing the activity of the positive feedback diverter, including modifying the switch or promoter in the positive feedback module to exhibit increased activity, or incorporating an additional copy of the positive feedback module. However, such modifications are expected to raise the basal levels of Ste4 at high pheromone input, potentially inhibiting the performance of the negative diverter. As an alternative strategy, we added a second module encoding constitutive expression of Ste4, or a booster module, to the positive feedback diverter to construct the amplifying diverter. Addition of the booster module has two notable advantages over a second feedback module. First, the booster module is insensitive to the resistance imposed by the negative diverter, such that Ste4 expression from this module is independent of the negative diverter's effect on pathway activity. Second, basal expression of Ste4 from the booster module is constant across the range of pheromone input, such that antagonization of the negative diverter does not increase from this module in the absence of its trigger molecule within the high-pheromone input regime. Thus, the incorporation of the booster module into the positive diverter architecture offers the potential to enhance the performance of the positive diverter, while imposing minimal effect on the performance of the negative diverter.

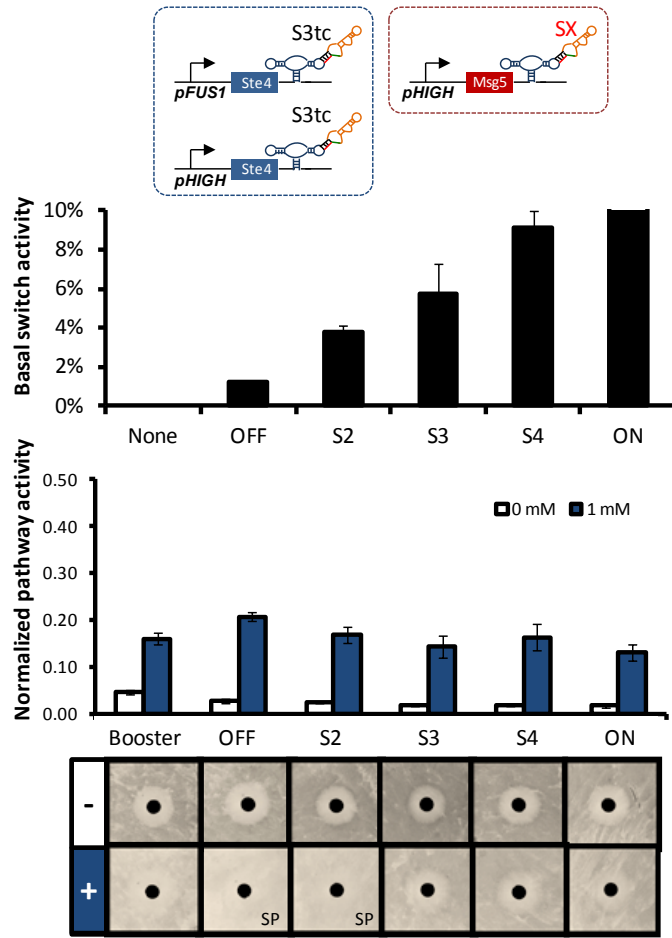


Figure 3.4. Addition of booster module to positive feedback diverter enhances fate switching in the presence of the resistance diverter. An amplifying diverter with S3tc regulating both expression modules is paired with resistance diverters incorporating pHIGH-Msg5 expression with switches of various activities. Pathway activation via this amplifying diverter diminishes as the basal activity of the resistance module increases. Networks constructed with this amplifying diverter and low Msg5 resistance (OFF, S2) show enhanced fate switching in halo assays relative to the booster diverter. However, for resistance modules with switch basal levels above S2 small-molecule triggered fate routing is weaker. “SP” denotes strong promiscuous routing in the plate assays.

The ability of the amplifying diverter to overcome antagonism from the negative diverter and achieve programmed routing to the promiscuous fate was examined. The amplifying diverter was composed of a tetracycline-responsive RNA switch regulating both expression modules (feedback: pFUS1-Ste4-S3tc; booster: pHIGH-Ste4-S3tc) and paired with resistance diverters incorporating a set of theophylline-responsive RNA switches exhibiting a range of activities (pHIGH-Msg5-Sx). Pathway activation and fate routing were evaluated as described previously. Results demonstrate that pathway

activation through the amplifying diverter diminishes as the basal activity of the resistance diverter increases (Figure 3.4). Network configurations with the amplifying diverter and low-strength resistance modules (i.e., OFF, S2) exhibit enhanced fate switching in halo assays relative to the booster module alone. Halo assays indicate that small-molecule-triggered routing to the promiscuous fate is noticeably weaker for resistance modules exhibiting greater activity. The data support that in the absence of the booster module, basal pathway activity in the presence of a resistance module is insufficient for amplification of pathway activity via the positive autoregulatory loop even in the presence of the molecular trigger (tetracycline). Thus, we postulate that increased expression from the booster module initiates increased pathway activity. Once the pathway activity crosses the requisite threshold, Ste4 expression is amplified and reinforced by the positive feedback module.

The pathway activation ratio (PAR) in the absence and presence of the environmental trigger provides a metric for evaluating a diverter's ability to facilitate cell fate reprogramming. A large PAR value is generally desirable for regulatory networks that route to divergent fates as it indicates a greater difference between the pathway activities of triggered and non-triggered cells. However, while the PAR value offers one performance metric for evaluating molecular network diverters, it is not a sufficient metric to determine a diverter's ability to route cells to an alternative fate. Diverters may achieve moderate PAR values by modifying basal pathway activity, but fail in routing if the triggered pathway activity does not cross the threshold for fate routing. Conversely, diverters exhibiting modest PAR values may effectively route fate provided they are

configured to cross the threshold of fate divergence. An optimal diverter configuration achieves both routing capability and a larger PAR value.

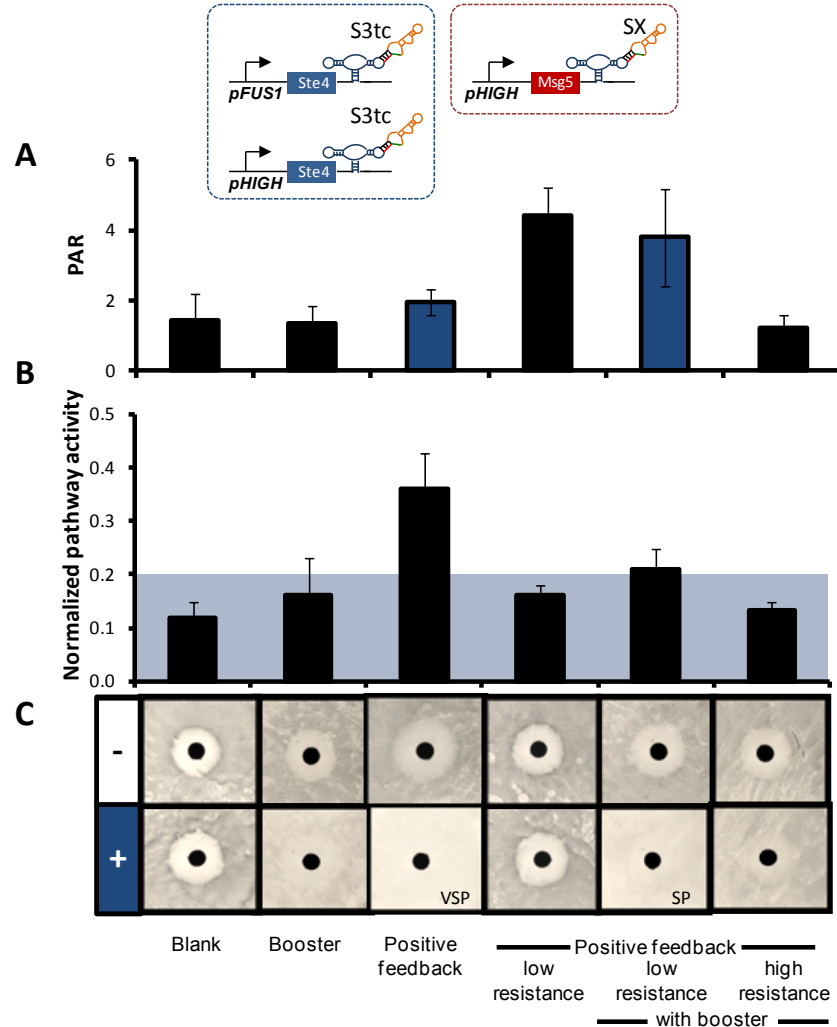


Figure 3.5. Pathway activation ratio is enhanced for positive feedback diverters in network configurations including a low-strength resistance module. A. Addition of a low strength resistance module to the synthetic network increases the PAR value of the positive feedback diverters with and without the booster module by lowering basal level expression. **B.** Pathway activity data for tetracycline triggered cells over a range of network configurations indicate that only two configurations sufficiently increase pathway activity above the requisite fate switching threshold. **C.** Halo assays demonstrate that only networks configured with the positive feedback modules (positive feedback diverter and amplifying diverter paired low resistance module) strongly route to the promiscuous fate. “SP” and “VSP” denote strong and very strong promiscuous routing in the plate assays, respectively.

The PAR values for positive diverters incorporating a variety of network configurations were determined by measuring the ratio of pathway activity in the presence and absence of the environmental trigger (tetracycline). Despite activating the

pathway sufficiently to route cells to the promiscuous fate, positive feedback diverter exhibits a lower PAR value due to the increased basal activity of the pathway associated with this diverter (Figure 3.5A). Further, the high basal pathway activity associated with the positive feedback diverter provides little resolution between the triggered and non-triggered populations (Figure 3.6A). The implementation of a positive feedback diverter with a low activity resistance diverter reduces the basal pathway activity, thereby increasing the PAR value for this network configuration and increasing population separation. However, the resistance module also suppresses amplification of pathway activity via the autoregulatory loop, thus inhibiting routing to the promiscuous fate (Figure 3.6B, Figure 3.5). Robust routing to the promiscuous fate is only achieved when a low activity resistance diverter is paired with an amplifying diverter (Figure 3.5B, C), resulting in enhanced separation between the triggered and non-triggered populations (Figure 3.6C). Altering the network configuration by incorporation of a high activity resistance diverter reduces the pathway activity, resulting in a diminished PAR value and weaker routing to the promiscuous fate. We postulate that the resistance module enhances differentiation between triggered and non-triggered populations by buffering the effect of subthreshold variations in Ste4 levels on pathway activity, reducing the amplification of noise in the system. Further, the strength of the resistance module modulates the triggered output from the amplifying diverter and thus tunes routing to the promiscuous fate. Therefore, the ability to rationally tune module and diverter activities is critical for configuring network architectures that can cross thresholds of fate divergence in the presence of environmental signals. Optimal diverter performance is enhanced by

networks that suppress noise amplification and other subthreshold variations in gene expression to robustly amplify the appropriate input.

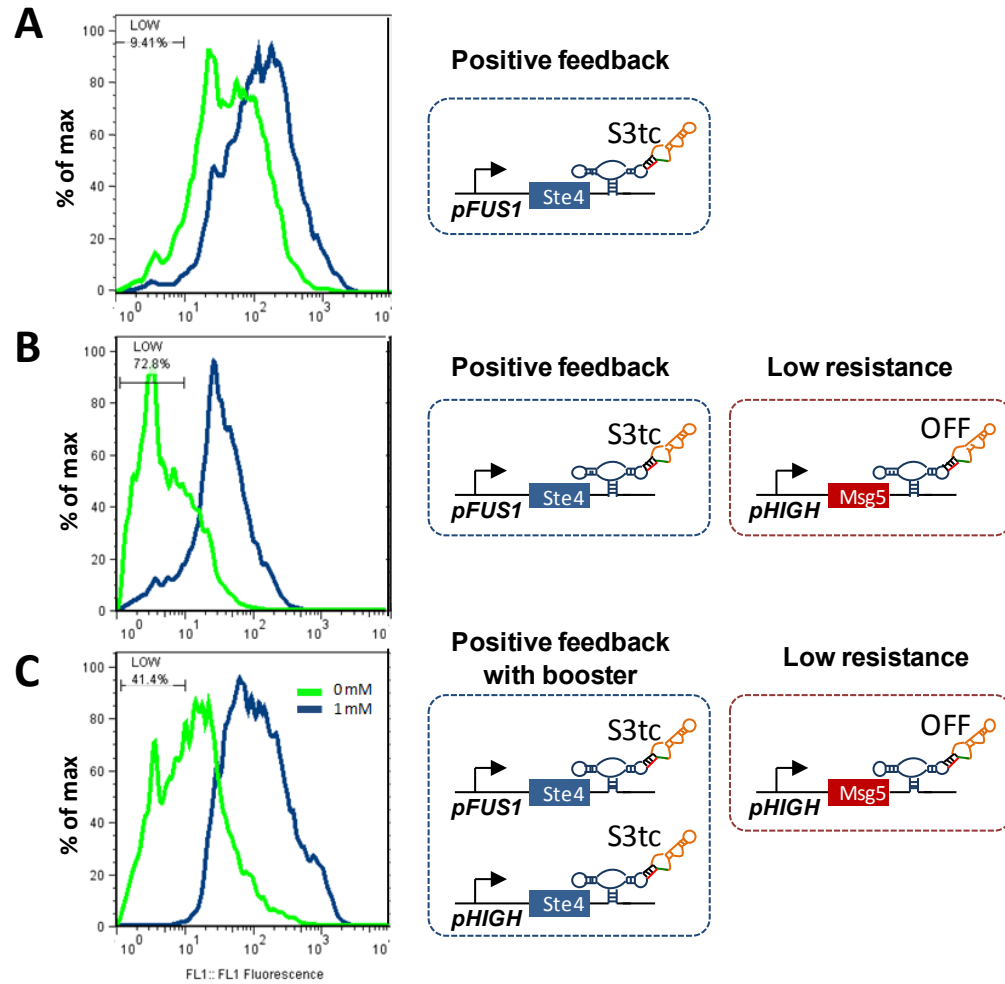


Figure 3.6. Structuring networks to amplify switching by layering positive feedback with a resistance module and a booster module. **A.** A histogram of pFUS1-GFP for the positive feedback diverter pFUS1-Ste4-S3tc shows significant overlap between the populations in the presence and in the absence of tetracycline, resulting in a low PAR value (1.9). Despite a low PAR value pFUS1-Ste4-S3tc effectively routes cells to the promiscuous fate (Figure 3.4). **B.** Adding the low resistance module to the network configuration via pHIGH-Msg5-OFF decreases overlap between the two populations, increasing the PAR value (4.4). Yet, this network provides insufficient pathway activation to route to the promiscuous fate when trigger with tetracycline (Figure 3.4). **C.** Addition of a booster module, pHIGH-Ste4-S3tc, to the positive diverter constructs the amplifying diverter. The booster module in the amplifying diverter boosts pathway activity, routing cells to the promiscuous fate when triggered. Further, population separation is maintained in this configuration as indicated by the high PAR value (3.8) (Figure 3.4).

Network configurations that balance positive feedback with negative feedback enhance pathway attenuation

While addition of the booster module enhances the ability of the positive diverter to route cells to the promiscuous fate, the increased basal expression from this amplifying diverter diminishes the ability of the resistance diverter to route cells to the chaste fate. We postulate that high levels of pheromone leads to amplification of the positive feedback loop, such that the positive diverter overwhelms the attenuation provided by the resistance diverter. Therefore, we examined the impact of adding a negative feedback module to this network to balance the pathway response.

To counteract the amplification of pathway activity via the positive feedback module in the amplifying diverter, we constructed an attenuating diverter, which incorporates a resistance module and a negative feedback module. An amplifying diverter was configured with a booster module that incorporated a strong tetracycline RNA switch (pHIGH-Ste4-S4tc) and a positive feedback module that incorporated a moderate tetracycline RNA switch (pFUS1-Ste4-S3tc). This amplifying diverter was paired with various attenuating diverters composed of a resistance module (pHIGH-Msg5-S3) and negative feedback modules incorporating a set of theophylline-responsive RNA switches exhibiting a range of activities (pFUS1-Msg5-Sx). Pathway activation and fate routing were evaluated as described previously. The results indicate that pathway attenuation is relatively insensitive to the strength of negative feedback module (Figure 3.7A). While GFP levels exhibit moderate changes with increasing negative feedback strength, halo assays indicate that these diverters robustly route cells to the chaste fate in the presence of theophylline above a threshold of negative feedback strength (S3, S4). In the absence

of theophylline, the network maintains normal halo formation for the negative feedback module regulated via S3. However, the network composed with the negative feedback module regulated by S4 exhibits reduced halo formation even in the absence of theophylline. The data indicate that there exists a threshold of negative feedback strength residing between the basal expression levels of S3 and S4 at which wild-type and chaste fates diverge.

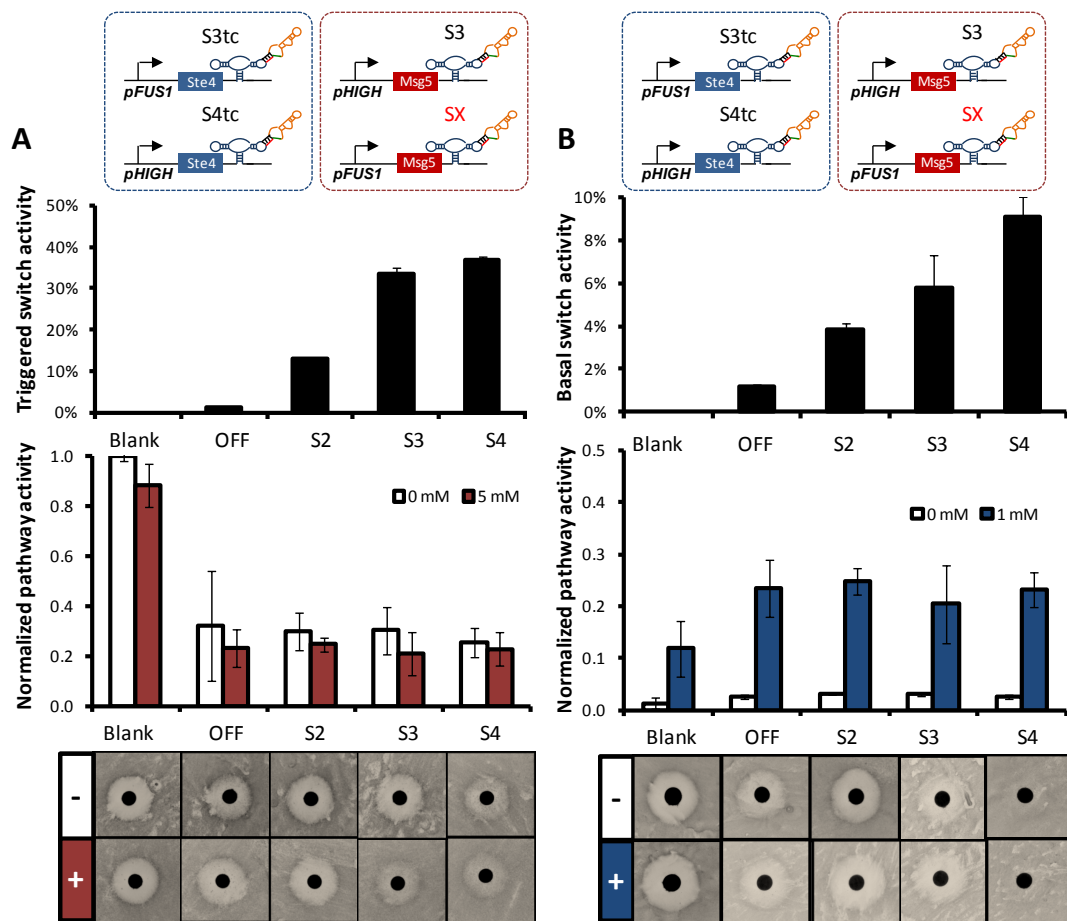


Figure 3.7. Networks configured with an amplifying diverter and various attenuating diverters show that pathway attenuation is a weak function of the strength of the negative feedback module. A. An amplifying diverter composed of pFUS1-Ste4-S3tc and pHIGH-Ste4-S4tc is paired with attenuating diverters incorporating pHIGH-Msg5-S3 and various strength negative feedback modules. While only modest changes are observed across the range of strengths for the negative feedback module, the attenuating diverter effectively routes to the chaste fate in the presence of the theophylline input when the active feedback strength of the negative diverter is at or above S3 levels. “SC” denotes strong chaste routing in the plate assays. **B.** The positive diverter weakly routes to the promiscuous fate in the presence of the tetracycline input when the basal feedback strength of the negative diverter is below S3. The basal feedback strength of S3 in the negative diverter is sufficient to inhibit the positive diverter.

The incorporation of an attenuating diverter, pairing both a resistance module and a negative feedback module, allowed chaste routing in the presence of the amplifying diverter. We next evaluated the ability of this dual diverter architecture to activate the pathway and route cells to the promiscuous fate in the presence of the positive diverter trigger over a range of negative feedback strengths. While GFP levels indicate that the amplifying diverter achieves moderate pathway activation within this network configuration, routing of fate to the promiscuous phenotype is weak across the range of negative feedback modules (Figure 3.7B). Based on these results, we chose to utilize a negative feedback module in the dual diverter architecture that provided strong chaste routing (pFUS1-Msg5-S3) as we examined tuning other components in the network to enhance pathway activation and routing to the promiscuous fate.

The performance of the amplifying and attenuating diverters in dual diverter networks are sensitive to the strength of the resistance module

To enhance routing to the promiscuous fate in the dual diverter network, we examined the impact of tuning the strength of the resistance module. The amplifying diverter (positive feedback: pFUS1-Ste4-S3tc; booster: pHIGH-Ste4-S4tc) was paired with attenuating diverters composed of a negative feedback module (pFUS1-Msg5-S3) and resistance modules incorporating RNA switches exhibiting a range of activities (pHIGH-Msg5-Sx). The performance and fate routing function of the dual diverter networks with varying resistance modules were characterized. For this dual diverter configuration, the amplifying diverter significantly increases pathway activity when

paired with weaker resistance modules (S2 and below). Pathway activation is reduced and the amplifying diverter is unable to strongly route cells to the promiscuous fate when paired with resistance modules of greater activity (S3 and above) (Figure 3.8). The results demonstrate that to preserve chaste routing the basal resistance activity must be between S2 and S3, indicating a threshold of resistance within this configuration that permits promiscuous routing via the amplifying diverter.

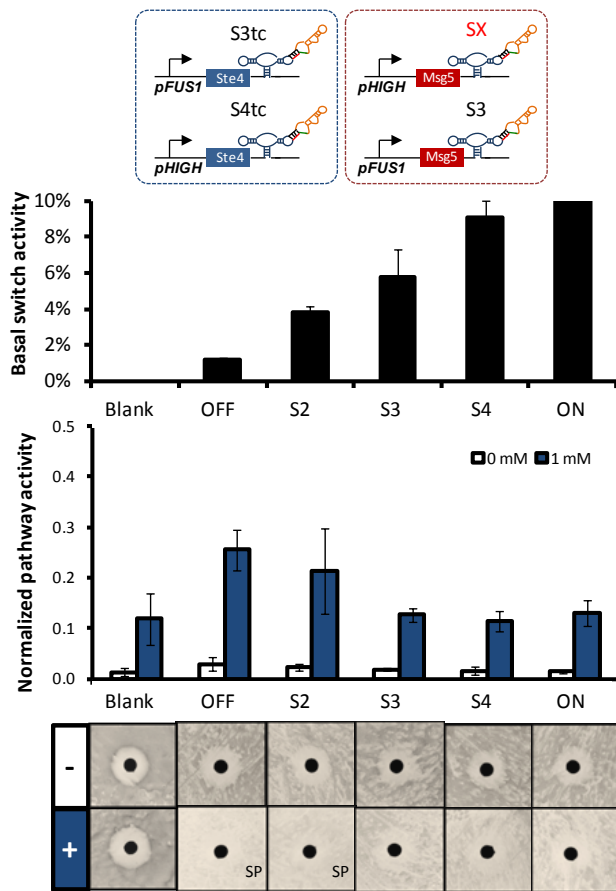


Figure 3.8. A dual-module positive diverter shows that pathway activation is sensitive to the activity of the resistance module. Amplifying diverter (positive feedback: pFUS1-Ste4-S3tc; booster: pHIGH-Ste4-S4tc) paired with various attenuating diverters (negative feedback: pFUS1-Msg5-S3; resistance: pHIGH-Msg5-Sx). “SP” denotes strong promiscuous routing in the plate assays.

We next evaluated the performance and fate routing of the attenuating diverter within the dual diverter network over varying resistance activities. The data demonstrate that pathway attenuation is sensitive to the activity of the resistance module (Figure 3.9).

Pathway activity drops as resistance increases from low to medium strength, above which the effect of resistance appears to saturate. Specifically, increasing the strength of resistance above that exhibited by the S3 module does not significantly reduce pathway activity. Strong chaste routing is observed in the presence of theophylline for resistance modules with activity at and above S3 levels. While no network configuration achieves dual-fate routing, the dual diverter network with S2 regulating the resistance module permits promiscuous routing while S3 enables chaste routing. These data indicate that dual-fate routing may be achieved by tuning the strength of the resistance module around the activation and attenuation thresholds that reside between S2 and S3.

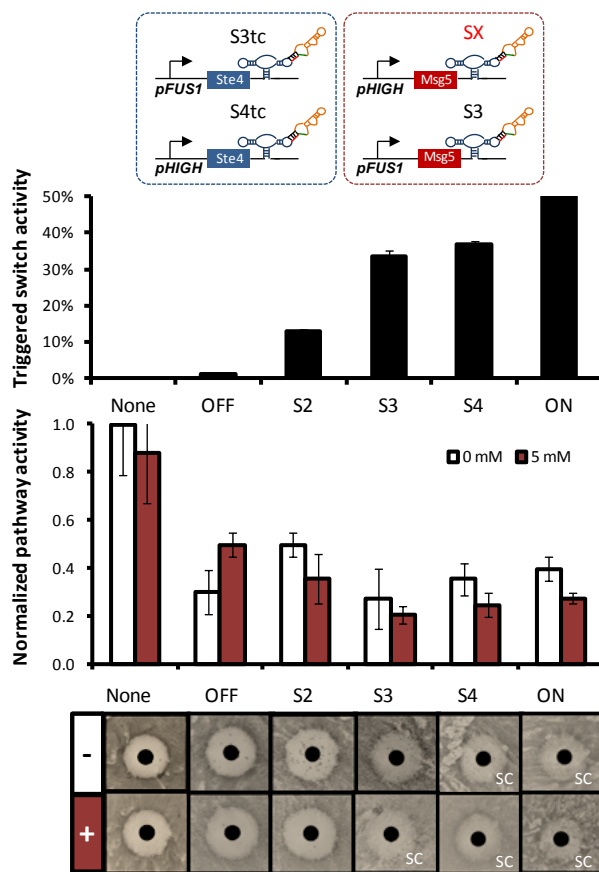


Figure 3.9. A dual-module negative diverter shows that pathway attenuation is a strong function of the activity of the resistance module. Amplifying diverter (positive feedback: pFUS1-Ste4-S3tc; booster: pHIGH-Ste4-S4tc) paired with various attenuating diverters (negative feedback: pFUS1-Msg5-Sx; resistance: pHIGH-Msg5-Sx). “SC” denotes strong chaste routing in the plate assays.

The performance of attenuating and amplifying diverters is sensitive to the strength of the positive feedback module

We also examined the impact of tuning the strength of the positive feedback module on the dual-routing capability of the dual diverter network configuration. The attenuating diverter (resistance: pHIGH-Msg5-S3; negative feedback: pFUS1-Msg5-S3) was paired with amplifying diverters composed of a booster module (pHIGH-Ste4-S4tc) and positive feedback modules incorporating sets of RNA switches exhibiting varying activities (pFUS1-Ste4-Sx). We evaluated the ability of the attenuating diverter to reduce pathway activity and route cells to the chaste fate in this network configuration. Pathway attenuation increases modestly with decreasing positive feedback strength from S4tc to S2tc (Figure 3.10A). Across the range of positive feedback modules incorporating S2tc to S4tc, wild-type halo formation is mostly maintained in the absence of theophylline. For the network incorporating the OFF state control within the positive feedback module, pathway activity is low and cells are strongly routed to the chaste fate even in the absence of theophylline. While decreasing the strength of the positive feedback module may improve chaste routing, the data indicate that within this network configuration positive feedback above a particular threshold is required to maintain halo formation in the absence of either small-molecule trigger.

We next evaluated the ability of the amplifying diverter to increase pathway activation in these networks over the range of positive feedback strengths. Pathway activation increases with increasing positive feedback strength from OFF to S2tc. Increasing positive feedback strength above S2tc did not result in significant changes to either pathway activation or promiscuous routing within this network configuration

(Figure 3.10B). However, the wild-type halo was diminished in the absence of tetracycline over the range of feedback strengths compared to the same assay conditions (Figure 3.10A and B). These data indicate that the dual diverters' ability to maintain the wild-type halo may be sensitive to small, unaccounted for variations in plating conditions such as humidity and temperature which may affect plate diffusivity and thus the pheromone gradient. We additionally investigated whether reducing the positive feedback strength from S3tc to S2tc enhanced dual-fate routing in the dual diverter network. Specifically, we paired the amplifying diverter (booster: pHIGH-Ste4-S4tc; positive feedback: pFUS1-Ste4-S2tc) with attenuating diverters composed of a negative feedback module (pFUS1-Msg5-S3) and resistance modules incorporating a set of RNA switches exhibiting a range of activities. While reducing the strength of the positive feedback module did enhance chaste routing for the dual diverter network, it also resulted in weaker promiscuous routing even when configured with low activity resistance modules (Supplementary Figure 3.3). Reducing the strength of the booster module (pHIGH-Ste4-S3tc) similarly resulted in weaker promiscuous routing in this network configuration without significantly improving routing to the chaste fate (Supplementary Figure 3.4). The results indicate that the strength of the positive feedback module represents a sensitive parameter in the dual diverter network that must be precisely tuned to allow robust function of the dual-routing activities.

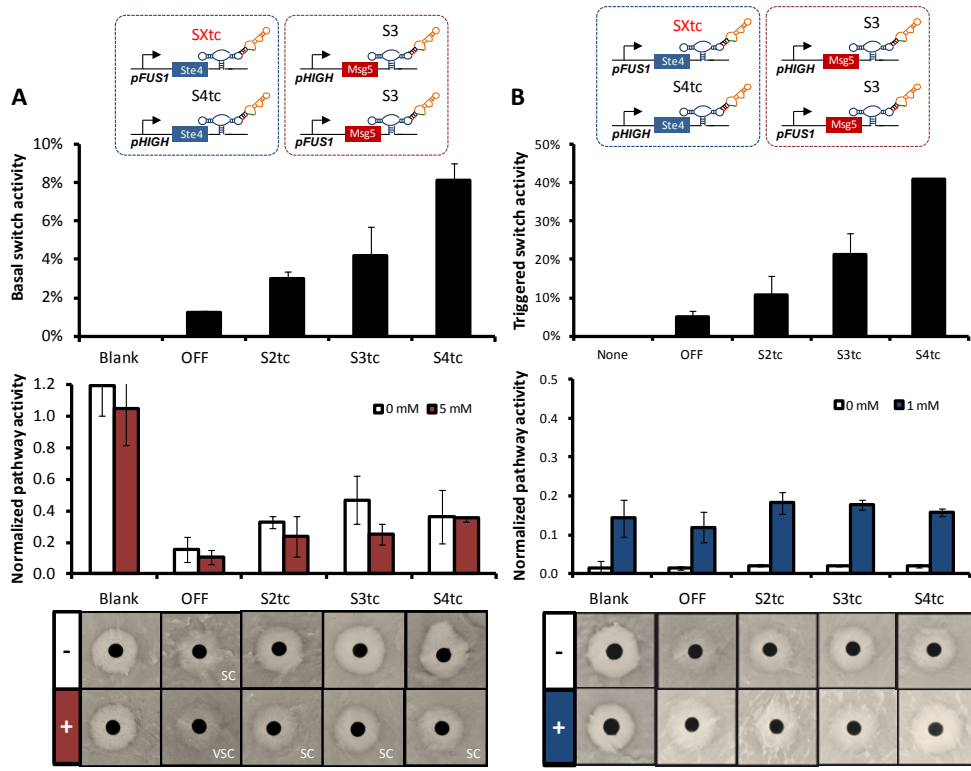


Figure 3.10. A dual-module negative diverter shows that pathway attenuation and activation are sensitive to the strength of the positive feedback module. A. Attenuating diverters (negative feedback: pFUS1-Msg5-S3; resistance: pHIGH-Msg5-S3) paired with various amplifying diverters (positive feedback: pFUS1-Ste4-SXtc; booster: pHIGH-Ste4-S4tc). “SC” and “VSC” denotes strong and very strong chaste routing in the plate assays, respectively. **B.** Pathway activation is relatively insensitive to varying positive feedback strength and only very weak routing is observed across the range of networks. However, insufficient levels of positive feedback in this network configuration inhibit normal halo formation in the absence of either trigger.

Benchmarking network diverter performance

Having examined a variety of network configurations, we identified several configurations that achieve near-optimal performance given our set of parts and the architectures we had constructed. We sought to benchmark four of the best dual-routing configurations to networks with reduced diverter antagonism. To benchmark performance of the dual diverter networks, we compared the routing efficiency and efficacy of the dual diverters to minimally antagonistic alternative architectures (MAAAs). MAAAs

represent best-case scenarios for routing under conditions of reduced interference from the opposing diverter. Six different MAAAs, three positive and three negative, were composed to evaluate the performance of both the positive and negative diverters in various configurations.

Positive MAAAs provide a tool for benchmarking a dual diverter's efficiency in activating the pathway and efficacy in routing to the promiscuous fate. Positive MAAAs are constructed by reducing the strength of modules within the negative diverter, thereby minimizing the antagonistic impact exerted by the negative diverter on the function of the positive diverter. We compared the constructed dual diverters to three different positive MAAAs: the low-resistance, the no-negative-feedback, and the low-resistance-no-negative-feedback MAAAs (For details of configuration see legend in Figure 3.11). We selected four dual diverter configurations that vary in the strength of positive feedback and resistance modules (positive feedback: pFUS1-pSte4-Sxtc; booster: pHIGH-Ste4-S4tc; negative feedback: pFUS1-Msg5-S3; resistance: pHIGH-Msg5-Sx). For simplicity, we refer to these dual diverters as: Diverter A, B, C, and D. Diverters A and B are composed with S3tc regulating the positive feedback module and the resistance module is regulated via S2 and S3, respectively. Diverters C and D mirror Diverters A and B, respectively, except S2tc is incorporated into the positive feedback module. These dual diverters are expected to decrease in positive routing and increase in negative routing performance from A to D.

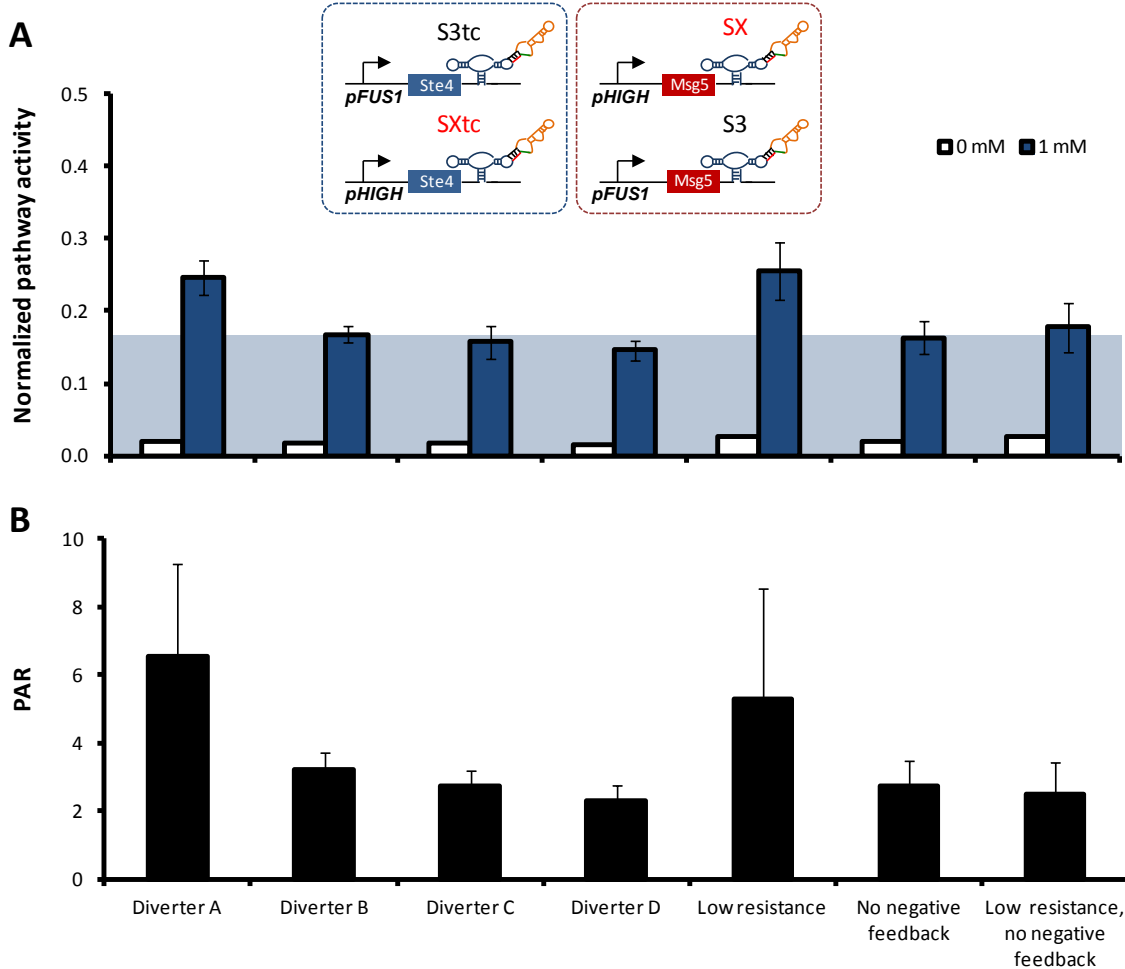


Figure 3.11. Benchmarking a dual diverters against various positive MAAs indicates strong performance by Diverter A. A. A. Diverter A performs as well as the low resistance MAAA in activating the pathway, while pathway activation is notably diminished for Diverters B through D. All four dual diverter networks utilize a negative feedback module regulated by S3 and a booster module regulated via S4tc. Diverter A and Diverter B are composed with S3tc regulating the positive feedback module and the resistance module is regulated via S2 and S3, respectively. Diverters C and Diverter D mirror Diverters A and B respectively with S2tc substituted for S3tc in the positive feedback module. All the MAAs containing the booster and negative feedback also have S4tc for the booster and S3 for negative feedback. Otherwise the MAAs were composed without these elements to minimize antagonization. B. PAR values indicate that Diverter A performs as well as the MAAs in differentiating the triggered and non-triggered populations, while performance drops for Diverter B and diminishes further across the range to Diverter D. The “low resistance” MAAA is composed with S3tc regulating positive feedback module, S4tc regulating the booster module, S3 regulating the negative feedback module and OFF regulating the resistance module. The low resistance MAAA represents the lowest possible level of resistance from this expression module given the other parameters (eg. strength of promoter, pathway regulator). The “no negative feedback” MAAA is composed similarly to the low resistance MAAA except it lacks a negative feedback module and contains S3 regulating the resistance module. The “no negative feedback, low resistance” MAAA lacks a negative feedback module and contains the OFF state control regulating the resistance module.

In evaluating positive routing, Diverter A performs as well as the low resistance MAAA in activating the pathway, while pathway activation is notably diminished for Diverters B through D (Figure 3.11A). As previously observed, pathway activation is particularly sensitive to the strength of resistance in the range between S2 and S3 when the positive feedback module is regulated by S3tc. Comparison of Diverters A and B with C and D reveals that decreasing the strength of the positive feedback module reduces this sensitivity by making the network less responsive to pathway activation. Interestingly, the positive MAAs lacking a feedback module showed reduced pathway activity relative to the low-resistance MAAA. While lower pathway activity values for the MAAs lacking a negative feedback module is unexpected, the differences in activity evaluated at a single time point may be the result of altered systems dynamics introduced by negative feedback. Negative autoregulation has been previously demonstrated to accelerate pathway response [25]. By evaluating a single time point of pathway activity, our assay may not capture an equally predictive measure of cellular fate when comparing different architectures. PAR values indicate that Diverter A performs as well as the low resistance MAAA in differentiating the triggered and non-triggered populations, while the PAR value drops for Diverter B and diminishes further in Diverters C and D (Figure 3.11B). While the PAR value for Diverter B (PAR 3.1) is lower than that for A (PAR 6.6) and the low-resistance MAAA, Diverter B outperforms the booster diverter (PAR 1.4) and positive feedback diverter (PAR 1.9) in differentiating triggered and non-triggered populations (Figure 3.4). These data indicate that with further tuning the constructed networks may provide strong resolution between divergent cell fates.

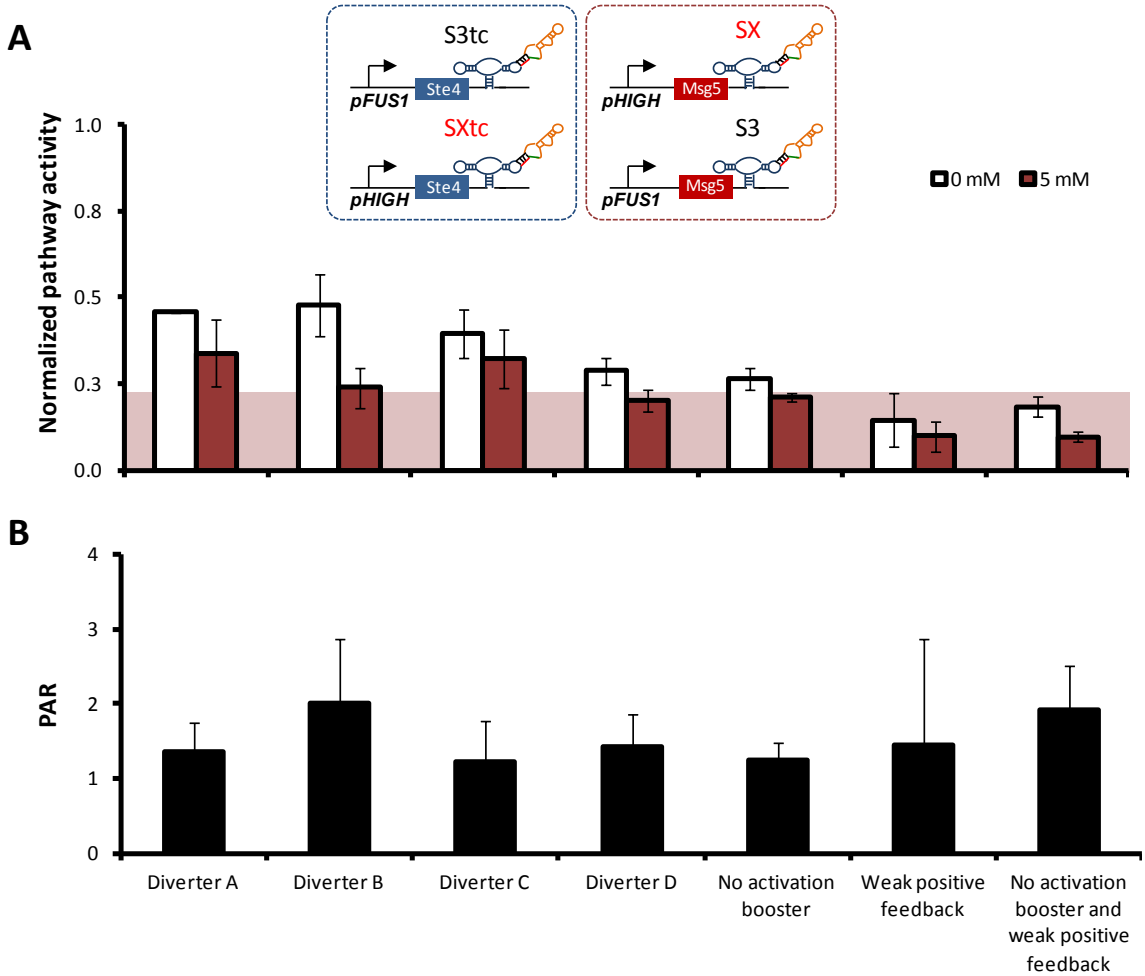


Figure 3.12. Benchmarking dual diverters against various negative MAAs indicates strong performance from Diverter B and D. **A.** Normalized pathway activity data shows that pathway attenuation for Diverter B and D is similar to the no activation booster control. The data indicate that to further reduce pathway activity requires reducing the strength of the positive feedback module to the OFF state control levels. However, this configuration inhibits pathway activity even in the absence of theophylline. As observed previously, for these dual diverter networks a minimal level of positive feedback is necessary to maintain wild-type halo formation in the absence of either small molecule. **B.** PAR values indicate that Diverter B performs as well as or better than the negative MAAs in separating triggered and non-triggered populations. The negative MAAs were composed with S3tc regulating the positive feedback module, S4tc regulating the booster module, S3 regulating both the negative feedback and resistance modules with the following changes to the positive diverter. In the “no-activation-booster” MAAA lacks a booster module. The “weak-positive-feedback” MAAA is composed with the OFF state control regulating the positive feedback module. The no-activation-booster-weak-positive-feedback” MAAA lacks a booster module and contains a positive feedback module regulated by the OFF state control.

To benchmark the dual diverter’s efficiency in pathway attenuation and efficacy of routing to the chaste fate, we constructed three negative MAAs by reducing the strength of the expression modules in the positive diverter. We compared the four dual

diverters to the three negative MAAAs: no-activation-booster, weak-positive-feedback, and no-activation-booster-weak-positive-feedback MAAAs (For details of configuration see legend in Figure 3.12). When triggered with theophylline, pathway activation data shows that pathway attenuation for Diverters B and D is similar to the no activation booster control (Figure 3.12A). The data indicate that further reduction in pathway activity requires reducing the strength of the positive feedback module to levels exhibited by the OFF state control, which results in inhibition of pathway activity even in the absence of theophylline. As observed previously, a minimal level of positive feedback is necessary to maintain wild-type halo formation in the absence of either small-molecule trigger. From the measured PAR values, Diverter B performs as well as or better than the negative MAAAs in separating triggered and non-triggered populations (Figure 3.12B). The data indicate that configuring the dual diverter networks for differentiating between triggered and non-triggered cells and conditional chaste routing requires precise balancing of the positive feedback strength.

In comparing the various MAAAs and dual diverter configurations, Diverter B emerged as the best overall dual diverter. Diverter B achieved moderate levels of pathway activity and the second highest PAR value for pathway activation. Additionally, Diverter B attenuated pathway activity nearly as well as the no-booster MAAA and had a significantly higher PAR value for attenuation compared to the other dual diverters. While Diverter B represents the best overall dual diverter, Diverter A demonstrates that strong pathway activation can be achieved from the dual diverter architecture with amplifying and attenuating diverters simultaneously integrated. In addition, Diverter D demonstrates that strong pathway attenuation is possible from the same network

architecture tuned with different modular parts. Taken together, these results indicate that given the existing parts used in this study, we have optimized the dual routing system. Apart from modifying diverter configurations, further improvements in dual-fate routing may be achieved by increasing the trigger signals that activate the diverter switches and/or modifying growth conditions to modulate metabolic rate.

Conditional routing of genetically identical cells to diverse phenotypes in response to distinct molecular signals

We examined the performance of the dual diverters under conditions of elevated switch activation by examining dual-fate routing at elevated concentrations of the small-molecule triggers. Initial characterization of the dual diverter configurations were performed at extracellular concentrations of 5 mM theophylline and 1 mM tetracycline, which correspond to the standard concentrations for characterization of the RNA-based switches. However, increasing the concentration of small molecule input has been shown to increase the activation and thus level of expression from the RNA switches (Liang, J, et al. *Submitted*). To determine if increased activation of the theophylline- and tetracycline-responsive switches improved routing to the chaste and promiscuous fates, respectively, we performed halo assays in the absence and presence of slightly elevated concentrations of the environmental triggers (2 mM tetracycline, 20 mM theophylline). The results show that Diverters B, C, and D robustly route to the chaste fate when triggered with theophylline (Figure 3.13). Additionally, all four diverters modestly route cells to the promiscuous fate when triggered with tetracycline. However, Diverters B, C,

and D do not maintain wild-type halo formation in the absence of either trigger, instead demonstrating significant growth in the halo region in the absence of either trigger. We hypothesized that the positive diverter is overwhelmed by the negative diverter even at basal levels of expression resulting in reduced sensitivity to pheromone even in the absence of theophylline.

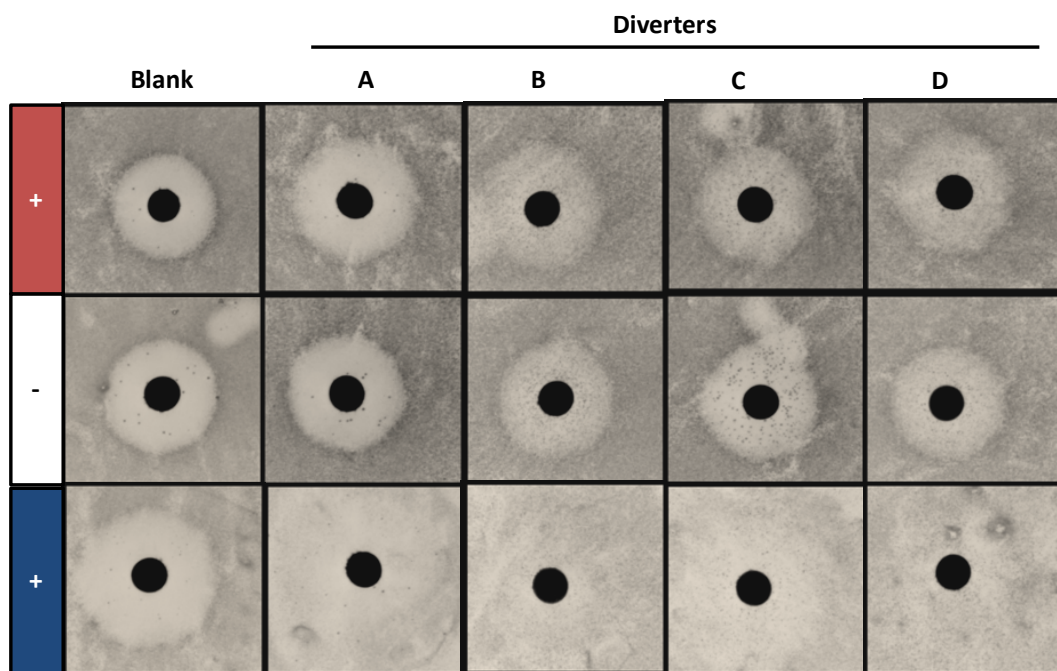


Figure 3.13. Higher small-molecule inputs improve dual-fate routing. Halo assays indicate that pushing the small-molecule concentration higher improves routing to both the promiscuous and chaste fate, but dual diverters routing to both fates (Diverters B, C, D) fail to maintain a robust wild-type halo in the absence of either trigger.

We attempted to restore the wild-type response in our dual diverters by altering growth conditions to support the positive diverter. Previous work demonstrated that the stability of positive feedback loops is sensitive to cellular metabolism [11]. In particular, reducing metabolism by exchange of sugar sources was shown to allow positive feedback loops to maintain memory of transient stimuli whereas under rapid growth conditions memory was lost. From this example, we postulated that noninducing, nonrepressing

(NINR) conditions, which are known to reduce metabolism compared to growth in dextrose, would support the positive feedback loop and restore the wild-type halo in the absence of either trigger. For all four diverters, the wild-type halo was restored in NINR conditions (Figure 3.14). Further, NINR conditions enhance promiscuous routing in the presence of tetracycline.

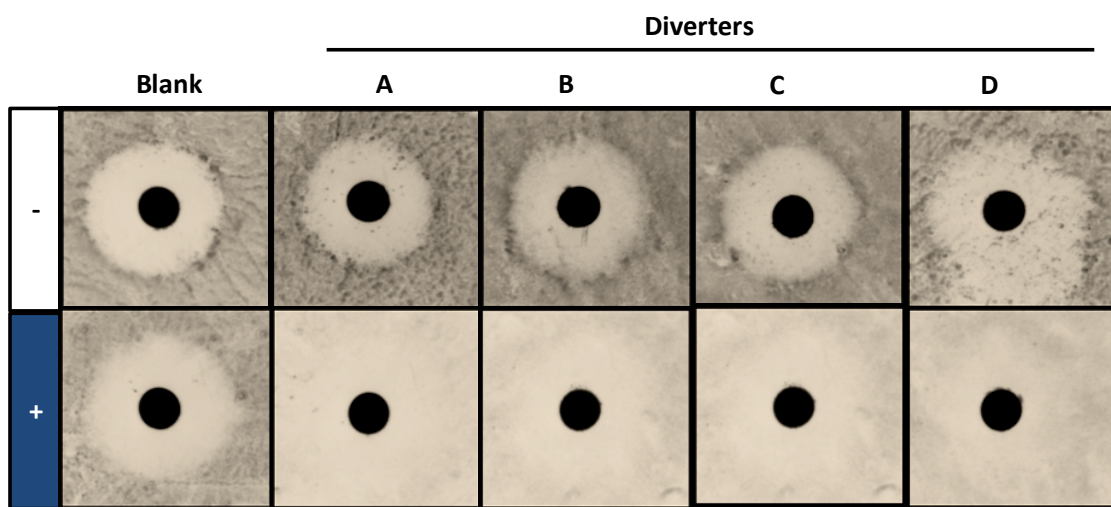


Figure 3.14. Metabolic modulation restores wild-type halo in the absence of either trigger and enhances promiscuous fate routing from dual-diverters. Halo assays performed in noninducing, nonrepressing (NINR) conditions demonstrate wild-type halos in the absence of either trigger. Assay performed at 0 mM (-) and 2 mM (+) tetracycline.

We further evaluated Diverter B, which emerged from the benchmarking as the best overall performing dual diverter, for dual routing at elevated small molecule levels supported by metabolic cues. As expected in NINR conditions, Diverter B maintains the wild-type halo until triggered by tetracycline to route cells to the promiscuous fate (Figure 3.15). When triggered with theophylline in dextrose, Diverter B routes cells to the chaste fate. Taken together, these data demonstrate that a dual diverter system has been optimized to achieve robust dual-fate routing from genetically identical cells in response to small-molecule triggers when supported by the appropriate metabolic cues.

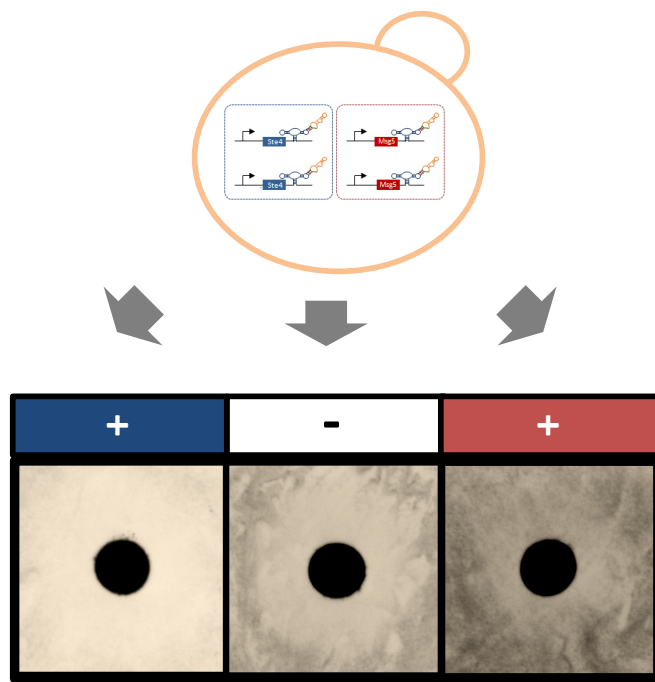


Figure 3.15. Routing genetically identical cells to divergent fates in response to small-molecule triggers supported by metabolic cues. Diverter B robustly routes cells to the promiscuous fate in response to tetracycline (left), preserved wild-type halo in absence of either trigger (center), and routes to the chaste fate in response to theophylline (right). Routing to the chaste fate is supported by dextrose, while wild-type and promiscuous fates are supported by NINR conditions.

Discussion

We have shown that molecular network diverters are capable of routing genetically identical cells to three divergent fates in response to specific environmental triggers when supported by metabolic modulation. The initial network configurations integrated single-module molecular network diverters, which had been previously optimized to route cell fate in the absence of the opposing diverter. Integration of the positive feedback diverter with the resistance diverter failed to permit dual-fate routing, and the basal expression levels from the opposing diverter resulted in antagonization, ultimately limiting the routing ability of each diverter. Addition of a booster module to the positive feedback diverter resulted in an amplifying diverter, which restored

promiscuous routing under low resistance conditions. In particular, the amplifying diverter paired with a low activity resistance module resulted in enhanced resolution between the triggered and non-triggered populations compared to the positive feedback diverter. Balancing the dual diverter networks with a negative feedback module facilitated routing to the chaste fate for some configurations at the sacrifice of promiscuous routing. By examining the network sensitivity to various parameters, our studies revealed that the strength of the positive feedback module and the activity of the resistance module represent highly sensitive control points. Our studies highlight the importance of architectures that allow for precise tuning of the diverter modules to allow dual fate routing. At lower levels of the environmental triggers none of the dual diverter networks achieved robust routing to both the promiscuous and chaste fates. However, under higher concentrations of the input triggers supported by metabolic modulation, a dual diverter configuration showed strong routing to both alternative fates while preserving the wild-type behavior in the absence of either trigger.

While we have optimized the dual diverter networks within the limits of the existing set of RNA switches, there remain potential opportunities for improving dual-fate routing performance. Given the sensitivity of the composed networks to the strength of the positive feedback module and the resistance module, balancing the strength of these modules represents an important design point for constructing networks that effectively route to both alternative fates. Basal level reduction from these expression modules represents a potential opportunity for further tuning of these networks.

Reducing expression from the resistance module and positive feedback module via promoter exchange or by modifying the expression context by integration or vector

exchange will reduce diverter antagonism from the opposing diverter by reducing basal expression levels. We used the pathway activity data for the dual diverter networks and switch expression levels to model the effect of reducing expression of both modules by one third for the Diverter B configuration (Figure 3.14). The results predict that absolute pathway activation and attenuation as well as PAR values for positive routing are improved in the modeled system relative to the best overall dual diverter, Diverter B. Thus, reducing expression from these cassettes may represent a potential opportunity for optimizing the performance of this dual diverter network configuration. In addition, integration at various loci, including GAL2 and TRP1, has been shown to reduce expression by 30–35%, providing a potential mechanism for reducing expression and variability from these constructs (Supplementary Figure 3.5). Promoter exchange represents another option for reducing expression from these modules. While there exist a variety of constitutive promoters with strengths lower than pHIGH, replacing a specific feedback promoter for variants of different strength may represent more of a challenge. However, previous work was performed to engineer variants of the mating promoter used in our study, pFUS1, that exhibit varying strengths of expression [26]. Several of the promoters demonstrated reduced strength and may be potential candidates for replacing the wild-type sequence used in these studies to reduce basal expression levels and enhance routing. While strategies that utilize promoter exchange or different expression contexts to tune basal levels will also result in reductions in the triggered levels of expression, addition of trans-acting controller may reduce basal expression without significantly reducing triggered expression.

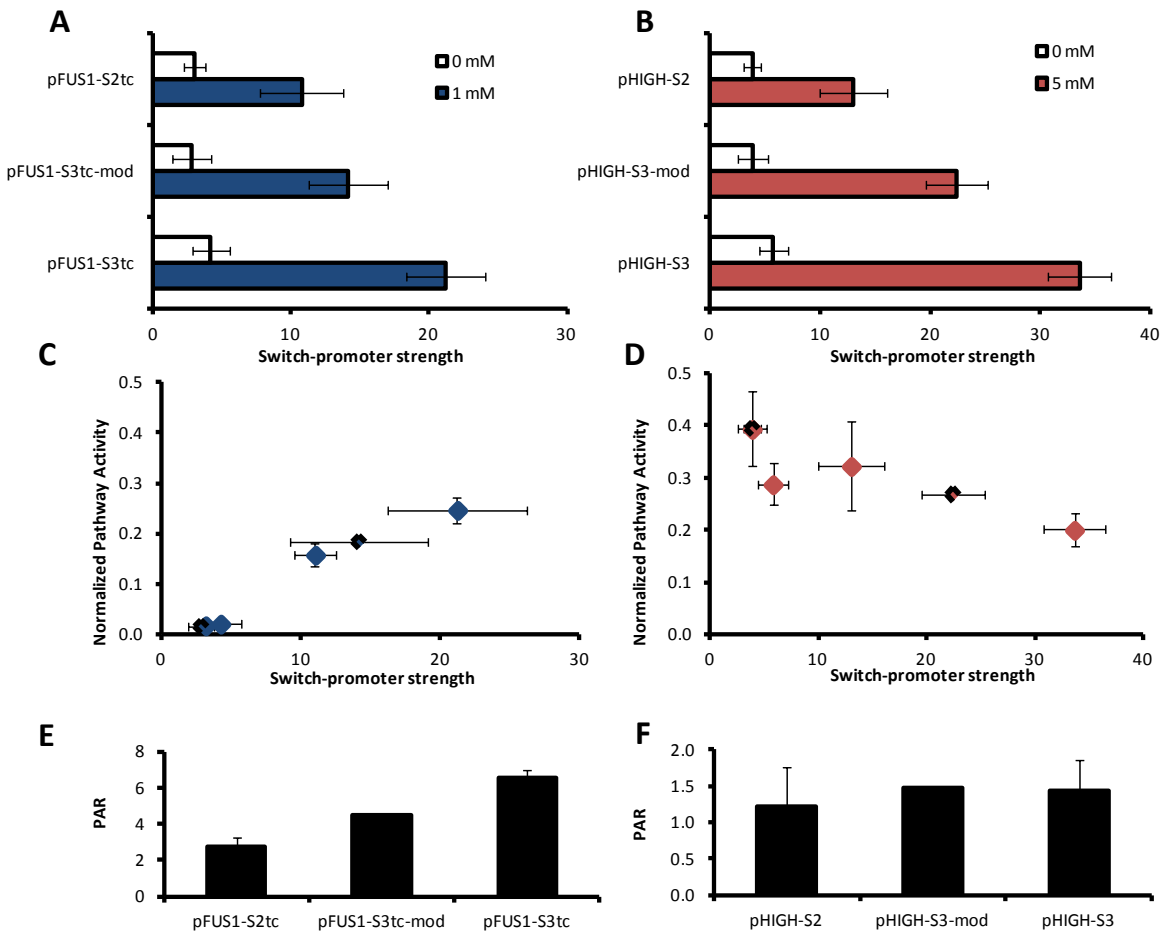


Figure 3.16. Reducing expression from the positive feedback and resistance modules in Diverter B may optimize the dual diverter network. **A.** Reducing expression from the feedback module by one third shifts the basal promoter-switch strength from S3tc levels to S2tc levels. pFUS1-S2tc denotes the feedback promoter combined with S2tc, pFUS1-S3tc denotes the feedback promoter with S3tc, and pFUS1-S3tc-mod indicates the promoter-switch strength for pFUS1-S3tc calculated to be reduced by one third. **B.** Reducing the resistance module by one third shifts basal levels from S3 to S2 levels. pHIGH-S2tc denotes the pHIGH promoter combined with S2tc, pHIGH-S3tc denotes pHIGH promoter with S3tc, and pHIGH-S3tc-mod indicates the promoter-switch strength for pFUS1-S3tc calculated to be reduced by one third. **C.** Pathway activity data are plotted in blue diamonds for pFUS1-S3tc (Diverter A) and pFUS1-S2tc (Diverter C) which both contain a resistance module regulated by S2. Diverter B contains a positive feedback module regulated via S3tc, a resistance module regulated via S3, a booster regulated via S4tc, and a negative feedback module. Pathway activity for the modified Diverter B was estimated by linearly interpolating between the values of pathway activity for pFUS1-S3tc (Diverter A) and pFUS1-S2tc (Diverter C) values of pathway activity, diamonds. **D.** Pathway activity data are plotted in red diamonds pHIGH-S2 (Diverter C) and pHIGH-S3 (Diverter D); both diverters contain S2tc regulating the positive feedback module. Pathway activity for the modified Diverter B was estimated by linearly interpolating between the values of pathway activity for pHIGH-S2 (Diverter C) and pHIGH-S3 (Diverter D), black diamonds. **E.** PAR values for pathway activation were determined from the measured and estimated values of pathway activity for the various configurations as previously described. **F.** PAR values for pathway attenuation for the various configurations were calculated using from measured and estimated values of pathway activity.

Trans-acting regulators of expression may provide a means for reducing basal expression levels, while being structured for minimal impact on the levels of triggered expression. Trans-acting RNA-based regulators, such as microRNAs or trans-acting ribozymes, offer a secondary layer of control by which to reduce basal level antagonization. Layering of trans-acting RNAs has been demonstrated to control basal level leakage, improving the performance of synthetic circuits [5, 12, 13]. Imbedding trans-acting RNA-based regulators within the transcripts of opposing regulators may facilitate the construction of mutually inhibitory loops between the two diverters. Such mutually inhibitory loops may be expected to increase the degree of divergence between cell fates and enhance the robustness of routing. Additionally, trans-acting RNA-based switches have been demonstrated to conditionally regulate target expression in mammalian cells [27]. Potentially, such trans-acting regulatory tools could provide a mechanism to conditionally reduce basal level expression with minimal effect on the triggered levels of expression. In addition to routing cells to three divergent fates, our work has demonstrated design principles for structuring networks to differentiate cells based on environmental cues and enhance the robustness of integrated mutually antagonistic programs. The dual diverter configurations incorporating the amplifying and attenuating diverters are structured to enhance routing while minimizing impact on performance of the opposing diverter. Achieving this effect required constructing functionally redundant genes with differential regulatory regions. Differential regulation of functionally redundant parts is a strategy that has been observed in natural biological systems, such as in the networks regulating bone formation and osteoblast differentiation as well as plant defense mechanisms and metabolism [28, 29]. Differential regulation of

functionally redundant genes may represent a common motif for amplifying pathway response to environmental cues that mediate changes in particular cellular behaviors and fate. Within our synthetic systems, we also observed that addition of a resistance module to the positive feedback diverter enhanced the resolution between the two populations of cells by reducing basal expression levels. We postulate that the resistance module enabled greater separation of the populations by buffering subthreshold noise of Ste4 expression. Addition of the booster module increased the levels of pathway activity in the network while preserving population resolution, providing a parameter for tuning the network output in this system. Synthetic networks that are structured to suppress noise amplification while amplifying differences in exogenous input may improve the selection of new RNA-based controllers by enhancing the resolution between switching and nonswitching elements. Additionally, when applied to cellular decision-making pathways, these enhanced amplifying circuits may facilitate robust differentiation between divergent cell fates.

We have demonstrated a scalable, modular, and tunable method for constructing RNA-based control systems that interact with a native signaling pathway to direct cell fate that may be readily translated to new pathways. As the synthetic biology tool box continues to expand, an increasingly number of synthetic control systems will be connected to native pathways, enabling more sophisticated and complex control for a wide array of applications. Many of the goals tissue engineering and molecular medicine such as the *ex vivo* construction of immunologically compatible tissues and the development of cell-based therapies will be advanced by synthetic control systems that spatially and temporally program cell fate.

Materials and methods

Plasmid construction

Standard molecular biology cloning techniques were used to construct all plasmids [30]. DNA synthesis was performed by Integrated DNA Technologies (Coralville, IA). All enzymes, including restriction enzymes and ligases, were obtained through New England Biolabs (Ipswich, MA). Ligation products were electroporated with a GenePulser XCell (Bio-Rad, Hercules, CA) into an *E. coli* DH10B strain (Invitrogen, Carlsbad, CA), where cells harboring cloned plasmids were maintained in Luria-Bertani media containing 50 mg/ml ampicillin (EMD Chemicals). All cloned constructs were sequence verified by Laragen Inc (Santa Monica, CA).

To construct the dual expression module negative and positive molecular network diverters, expression modules were cloned into dual cassette plasmids pCS2094 (Liang, J, et al. *Submitted*). pCS2094 served as the expression plasmid for positive feedback expression modules and resistance expression modules (Supplementary Figure 3.6A, Supplementary Table 3.1). The positive feedback expression module (pFUS1-Ste4-S2tc) was amplified via PCR with primers pFUS1.ClaI.pCS2094.FWD (5'-CCAATCTCAGAGGCTGAGTCTC) and Switch3'.XhoI.pCS2094.REV (5'-AAAACCTCGAGTTTATTCTTTGCTGTTCG) and cloned into the unique ClaI and XhoI sites in pCS2094 to construct pKG227 (Supplementary Figure 3.6B). Tetracycline-responsive switches and appropriate controls (Supplementary Table 3.5) were inserted into the 3' UTR via the unique restriction sites AvrII and XhoI, located immediately downstream of the Ste4 stop codon as described previously [31]. Resistance expression modules (pTEF7-Msg5-SX) were PCR amplified from previously constructed

single-module molecule network diverter plasmids (Supplementary Table 2.6) using pTEF7.FWD (5'-AAGAGCTCATAGCTTCAAAATGTCTCTACTCCTTTT) and CYC1t.NotI.REV (5'-AAAAGCGGCCGCTATATTACCCCTGTTATCC) and cloned into the unique restriction sites SacI and NotI of construct harboring the positive feedback expression modules (Supplementary Table 3.2). To construct a complimentary expression system to pCS2094 (-URA) for expression of negative feedback expression modules and booster expression modules a secondary -TRP plasmid with dual expression cassettes was constructed. pKG233, a pCS2094 based-plasmid, was digested with SacI and KpnI, the dual-cassette fragment was gel extracted, and inserted via these same unique restriction sites in pCS1128 to compose pKG243 (Supplementary Figure 3.6C). Negative feedback expression modules (pFUS1-Msg5-SX) were constructed by PCR amplifying Msg5 and theophylline switches from previously constructed single-module negative feedback diverter plasmids (Supplementary Table 2.7) using Msg5.K2.FWD (5'-AAAGGATCCAATTAATAGTGCACATGCAATTCAC) and Switch3'.XhoI.pCS2094.REV and cloned via the unique sites BamHI and XhoI. Booster expression modules (pTEF7-Ste4-SXtc) were added to the plasmids bearing the negative feedback expression modules via PCR of previously constructed booster diverter plasmids with pTEF7.FWD and CYC1t.NotI.REV and cloned into the unique restriction sites SacI and NotI (Supplementary Table 3.2). Single-module booster expression plasmids were constructed from pCS1128 for pairing with pCS2094. Previously constructed booster diverter plasmids were SacI and KpnI digested, the expression cassette was gel extracted, and cloned via these same unique restriction sites in pCS1128 (Supplementary Table 3.3).

Measuring mating pathway activity via a transcriptional reporter

The molecular diverter plasmids and appropriate controls were transformed into the previously constructed yeast mating reporter strain CSY840 (Supplementary Figure 3.9). Cells were inoculated into the appropriate dropout media, grown overnight at 30°C, and back diluted into fresh media in the presence or absence of ligand at the specified concentration to an OD₆₀₀ of <0.1. For negative diverters, after growing for 3 hr at 30°C, cells were stimulated with saturating pheromone levels, to a final concentration of 100 nM α mating factor acetate salt (Sigma-Aldrich, St. Louis, MO), to activate the mating pathway. Following 6 hr of growth post-back-dilution, GFP fluorescence levels from the pFUS1-yEGFP3 reporter were evaluated via flow cytometry using Cell Lab Quanta SC flow cytometer (Beckman Coulter, Fullerton, CA) with the following settings: 488-nm laser line, 525-nm bandpass filter, and photomultiplier tube setting of 5.0 on FL1 (GFP). Fluorescence data were collected under low flow rates for ~ 10,000 viable cells. Normalized pathway activity is calculated as the geometric mean of three biological replicates of each sample normalized to the blank plasmid control stimulated with saturating α mating factor in the absence of either small molecule.

Measuring mating pathway activity via halo assays

Mating associated cell-cycle arrest was evaluated via halo assays [32]. Halo assays were performed on cultures grown overnight in YNB with 2% dextrose or in 1% sucrose, 2% raffinose for NINR noninducing, nonrepressing (NINR) conditions and appropriate dropout solution. Overnight cultures were back diluted into fresh media and

grown to OD 600 ~ 0.2–0.4. 200 μ l of each replicate were plated on the appropriate dropout plates containing no small molecule, theophylline or tetracycline at the specified concentration on dextrose except where specifically indicated for NINR conditions. Standard concentrations are defined as 5 mM for theophylline and 1mM for tetracycline. After plating the cells, a gradient of α mating factor was established by saturating a filter disk (2 mm diameter) of Whatman paper with 9 μ l of 0.1 mg/mL α mating factor and placing the disk on the center of the plate. Cells were grown for 18–24 hr at 30°C and imaged via epi-white illumination with a GelDoc XR+ System (Bio-Rad).

Acknowledgements

Thanks to Joe Liang for plasmid pCS2094 as well as technical advice in incorporating and characterizing various switches into the molecular network diverters. Funding provided by the National Institutes of Health (R01GM086663).

References

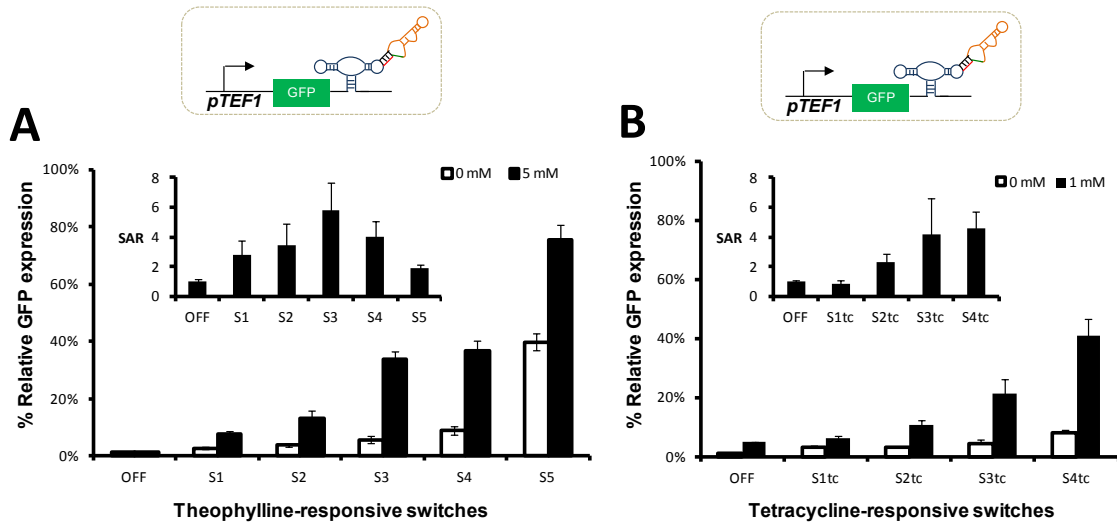
1. Perez-Moreno M, Fuchs E: **Catenins: keeping cells from getting their signals crossed.** *Dev Cell* 2006, **11**:601-612.
2. King TJ, Lampe PD: **Temporal regulation of connexin phosphorylation in embryonic and adult tissues.** *Biochim Biophys Acta* 2005, **1719**:24-35.
3. Schiller M, Javelaud D, Mauviel A: **TGF-beta-induced SMAD signaling and gene regulation: consequences for extracellular matrix remodeling and wound healing.** *J Dermatol Sci* 2004, **35**:83-92.
4. Sanjuan MA, Milasta S, Green DR: **Toll-like receptor signaling in the lysosomal pathways.** *Immunol Rev* 2009, **227**:203-220.
5. Callura JM, Dwyer DJ, Isaacs FJ, Cantor CR, Collins JJ: **Tracking, tuning, and terminating microbial physiology using synthetic riboregulators.** *Proc Natl Acad Sci U S A* 2010, **107**:15898-15903.
6. Kobayashi H, Kaern M, Araki M, Chung K, Gardner TS, Cantor CR, Collins JJ: **Programmable cells: interfacing natural and engineered gene networks.** *Proc Natl Acad Sci U S A* 2004, **101**:8414-8419.
7. Purnick PE, Weiss R: **The second wave of synthetic biology: from modules to systems.** *Nat Rev Mol Cell Biol* 2009, **10**:410-422.
8. Win MN, Smolke CD: **A modular and extensible RNA-based gene-regulatory platform for engineering cellular function.** *Proc Natl Acad Sci U S A* 2007.
9. Gardner TS, Cantor CR, Collins JJ: **Construction of a genetic toggle switch in *Escherichia coli*.** *Nature* 2000, **403**:339-342.

10. Friedland AE, Lu TK, Wang X, Shi D, Church G, Collins JJ: **Synthetic gene networks that count.** *Science* 2009, **324**:1199-1202.
11. Ajo-Franklin CM, Drubin DA, Eskin JA, Gee EP, Landgraf D, Phillips I, Silver PA: **Rational design of memory in eukaryotic cells.** *Genes Dev* 2007, **21**:2271-2276.
12. Deans TL, Cantor CR, Collins JJ: **A tunable genetic switch based on RNAi and repressor proteins for regulating gene expression in mammalian cells.** *Cell* 2007, **130**:363-372.
13. Xie Z, Wroblewska L, Prochazka L, Weiss R, Benenson Y: **Multi-input RNAi-based logic circuit for identification of specific cancer cells.** *Science* 2011, **333**:1307-1311.
14. Ferrell JE, Xiong W: **Bistability in cell signaling: How to make continuous processes discontinuous, and reversible processes irreversible.** *Chaos* 2001, **11**:227-236.
15. Becskei A, Seraphin B, Serrano L: **Positive feedback in eukaryotic gene networks: cell differentiation by graded to binary response conversion.** *Embo J* 2001, **20**:2528-2535.
16. Becskei A, Serrano L: **Engineering stability in gene networks by autoregulation.** *Nature* 2000, **405**:590-593.
17. Mangan S, Itzkovitz S, Zaslaver A, Alon U: **The incoherent feed-forward loop accelerates the response-time of the gal system of Escherichia coli.** *J Mol Biol* 2006, **356**:1073-1081.

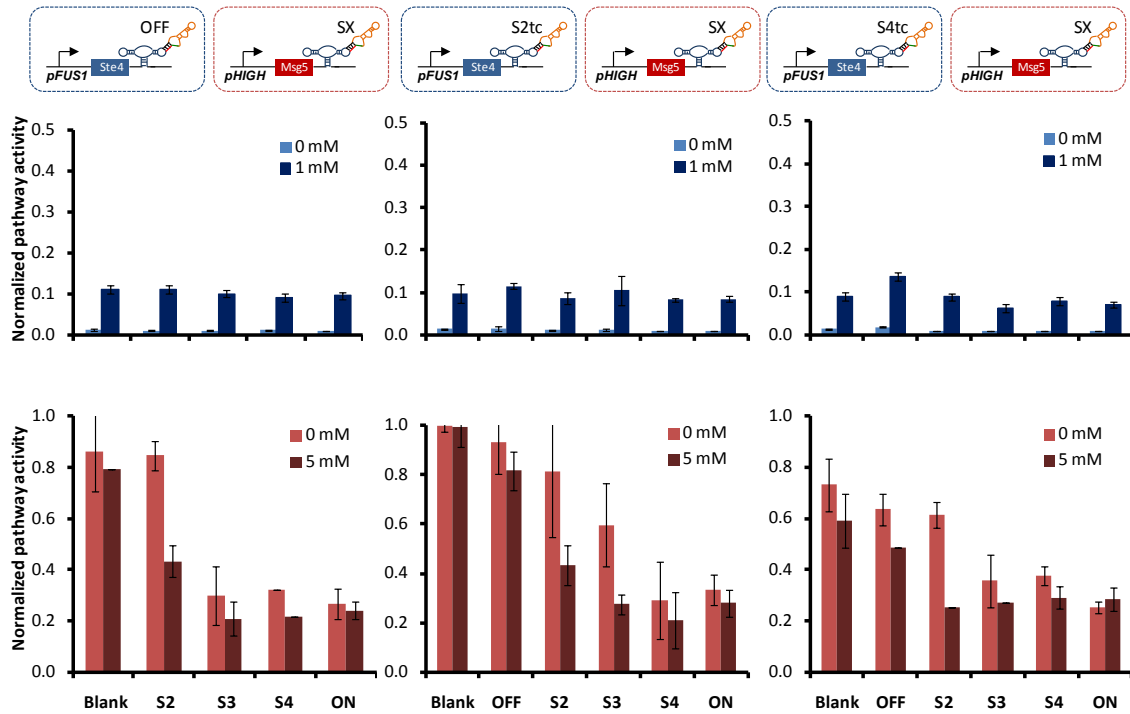
18. Mangan S, Alon U: **Structure and function of the feed-forward loop network motif.** *Proc Natl Acad Sci U S A* 2003, **100**:11980-11985.
19. Bashor CJ, Helman NC, Yan S, Lim WA: **Using engineered scaffold interactions to reshape MAP kinase pathway signaling dynamics.** *Science* 2008, **319**:1539-1543.
20. Ferrell JE, Jr.: **Self-perpetuating states in signal transduction: positive feedback, double-negative feedback and bistability.** *Curr Opin Cell Biol* 2002, **14**:140-148.
21. Ferrell JE, Jr., Pomerening JR, Kim SY, Trunnell NB, Xiong W, Huang CY, Machleder EM: **Simple, realistic models of complex biological processes: positive feedback and bistability in a cell fate switch and a cell cycle oscillator.** *FEBS Lett* 2009, **583**:3999-4005.
22. Xiong W, Ferrell JE, Jr.: **A positive-feedback-based bistable 'memory module' that governs a cell fate decision.** *Nature* 2003, **426**:460-465.
23. Espinosa-Soto C, Padilla-Longoria P, Alvarez-Buylla ER: **A gene regulatory network model for cell-fate determination during *Arabidopsis thaliana* flower development that is robust and recovers experimental gene expression profiles.** *Plant Cell* 2004, **16**:2923-2939.
24. Santos SD, Verveer PJ, Bastiaens PI: **Growth factor-induced MAPK network topology shapes Erk response determining PC-12 cell fate.** *Nat Cell Biol* 2007, **9**:324-330.
25. Rosenfeld N, Elowitz MB, Alon U: **Negative autoregulation speeds the response times of transcription networks.** *J Mol Biol* 2002, **323**:785-793.

26. Ingolia NT, Murray AW: **Positive-feedback loops as a flexible biological module.** *Curr Biol* 2007, **17**:668-677.
27. Beisel CL, Chen YY, Culler SJ, Hoff KG, Smolke CD: **Design of small molecule-responsive microRNAs based on structural requirements for Drosha processing.** *Nucleic Acids Res* 2011, **39**:2981-2994.
28. Banerjee C, Javed A, Choi JY, Green J, Rosen V, van Wijnen AJ, Stein JL, Lian JB, Stein GS: **Differential regulation of the two principal Runx2/Cbfa1 n-terminal isoforms in response to bone morphogenetic protein-2 during development of the osteoblast phenotype.** *Endocrinology* 2001, **142**:4026-4039.
29. Yuan Y, Chung JD, Fu X, Johnson VE, Ranjan P, Booth SL, Harding SA, Tsai CJ: **Alternative splicing and gene duplication differentially shaped the regulation of isochorismate synthase in Populus and Arabidopsis.** *Proc Natl Acad Sci U S A* 2009, **106**:22020-22025.
30. Sambrook J RD: *Molecular Cloning: A Laboratory Manual*, 3rd edn. Cold Spring Harbor, NY: Cold Spring Harbor Lab Press; 2001.
31. Win MN, Smolke CD: **A modular and extensible RNA-based gene-regulatory platform for engineering cellular function.** *Proceedings of the National Academy of Sciences* 2007, **104**:14283-14288.
32. Sprague GF, Jr.: **Assay of yeast mating reaction.** *Methods Enzymol* 1991, **194**:77-93.

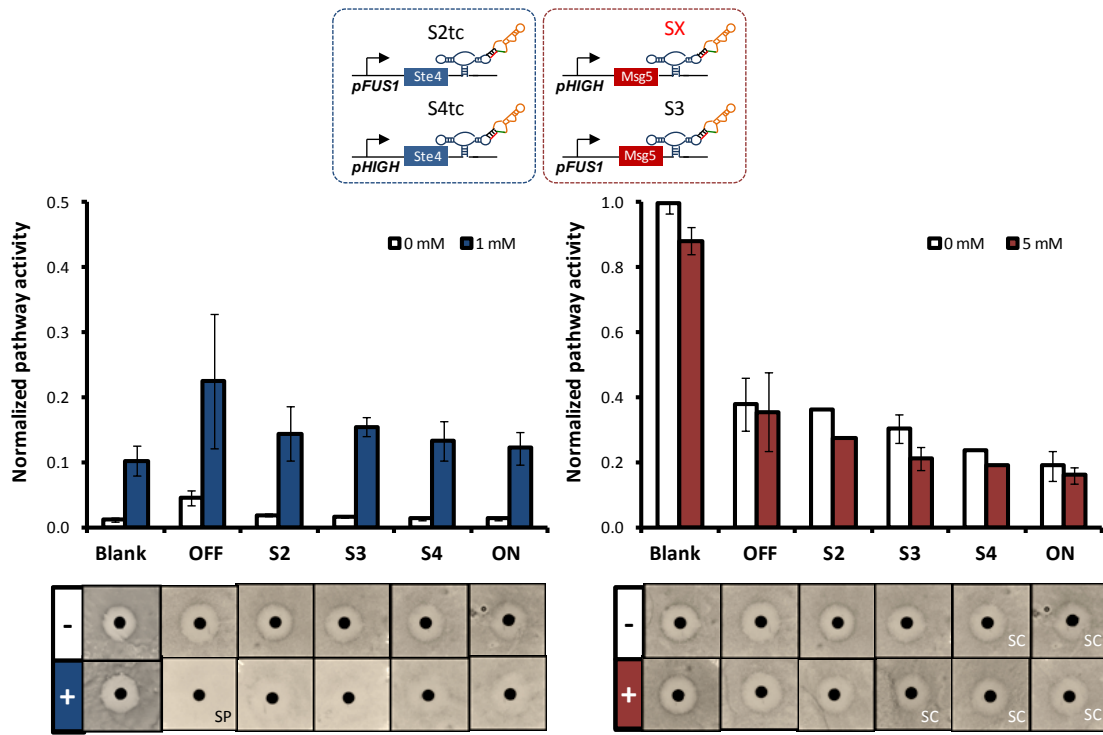
Supplementary figures



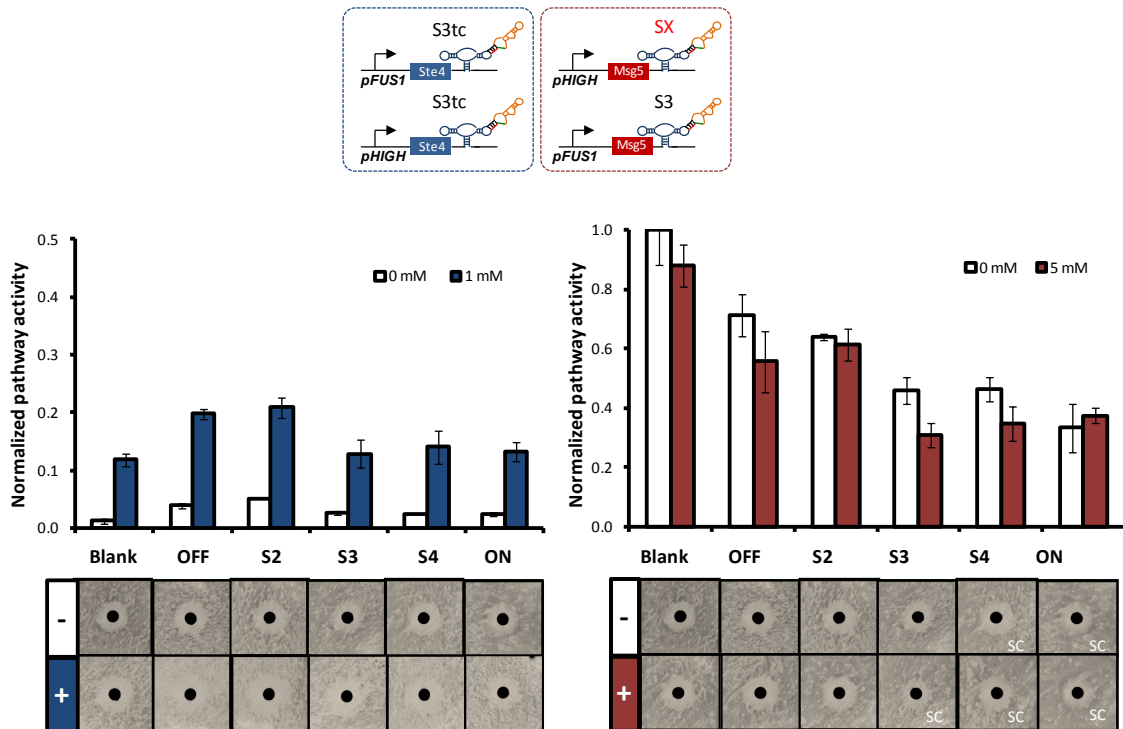
Supplementary Figure 3.1. Range of switch expression strengths. **A.** Theophylline-responsive switches' basal levels, the expression levels in the absence of ligand, range from 3% to 40% of the ON control. S3 has the highest switch activation ratio (SAR) at 5.7. SAR is the ratio of expression levels in the presence of ligand to the level in the absence of ligand. **B.** Tetracycline-responsive switches' basal levels range from 3% to 8%. S3tc and S4tc have similar high SARs at 5.2 and 5.1, respectively.



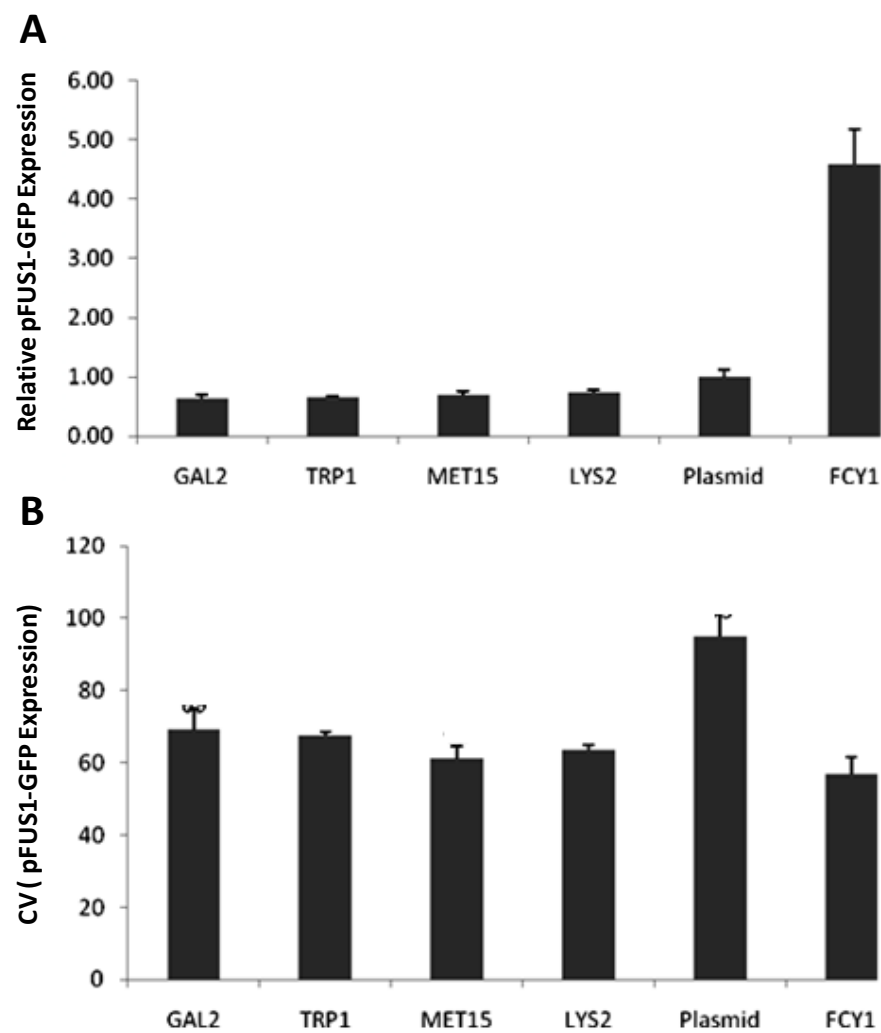
Supplementary Figure 3.2. Single-module diverters fail to achieve dual-fate routing. Single-module positive feedback diverters, pFUS1-Ste4 with OFF, S2tc, and S4tc, fail to route to the promiscuous fate in the presence of negative diverters incorporating a range of switch strengths. The Blank control bears a plasmid without either diverter.



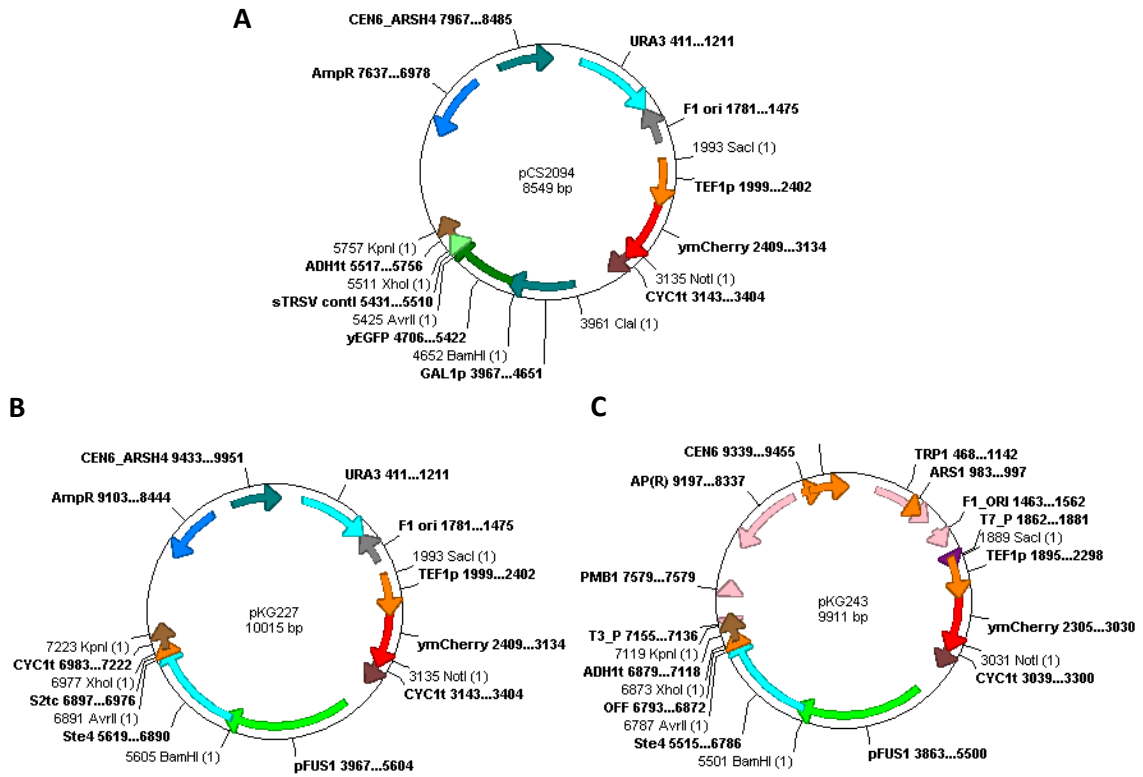
Supplementary Figure 3.3. Reducing the strength of the feedback module from S3tc to S2tc yields weak promiscuous routing while modestly improving chaste routing.



Supplementary Figure 3.4. Reducing the strength of the booster module from S4tc to S3tc yields weak promiscuous routing and does not significantly improve chaste routing.



Supplementary Figure 3.5. Loci characterization. **A.** Relative pFUS1-GFP expression indicates that integration generally reduces expression 25–35 % for the loci, except at the FCY1 locus which increases expression nearly 5-fold compared to the plasmid. The loci were characterized by flow cytometry of cells with pFUS1-GFP integrants stimulated with 100 nM for 3 hrs. **B.** Integration also reduced the coefficient of variation significantly.



Supplementary Figure 3.6. Plasmid maps: A. pCS2094 B. pKG227 C. pKG243

Supplementary tables

Supplementary Table 3.1. pCS2094-based dual-expression cassette plasmids

pCS #	pKG#	Downstream Cassette	Upstream Cassette	Marker
pCS2094	205	pTEF1-yEGFP-ON-CYC1t	pTEF1-mcherry-CYC1t	URA
	227	pFUS1-Ste4-S2tc	pTEF1-mcherry-CYC1t	URA
	306	pFUS1-Ste4-S2tc	pTEF7 Msg5 OFF	URA
	231	pFUS1-Ste4-S2tc	pTEF7 Msg5 S2	URA
	307	pFUS1-Ste4-S2tc	pTEF7 Msg5 S47	URA
	232	pFUS1-Ste4-S2tc	pTEF7 Msg5 S3	URA
	283	pFUS1-Ste4-S2tc	pTEF7 Msg5 ON	URA
pKG233		pFUS1-Ste4-OFF	pTEF1-mcherry-CYC1t	URA
pKG238		pFUS1-Ste4-OFF	pTEF7 Msg5 S2	URA
pKG300		pFUS1-Ste4-OFF	pTEF7 Msg5 S47	URA
pKG239		pFUS1-Ste4-OFF	pTEF7 Msg5 S3	URA
pKG271		pFUS1-Ste4-OFF	pTEF7 Msg5 ON	URA
pKG298		pFUS1-Ste4-Stc-OFF1	pTEF1-mcherry-CYC1t	URA
pKG302		pFUS1-Ste4-Stc-OFF1	pTEF7 Msg5 OFF	URA
pKG303		pFUS1-Ste4-Stc-OFF1	pTEF7 Msg5 S2	URA
pKG304		pFUS1-Ste4-Stc-OFF1	pTEF7 Msg5 S47	URA
pKG305		pFUS1-Ste4-Stc-OFF1	pTEF7 Msg5 S3	URA
pKG316		pFUS1-Ste4-Stc-OFF1	pTEF7 Msg5 ON	URA
pKG234		pFUS1-Ste4-S3tc	pTEF1-mcherry-CYC1t	URA
pKG310		pFUS1-Ste4-S3tc	pTEF7 Msg5 OFF	URA
pKG236		pFUS1-Ste4-S3tc	pTEF7 Msg5 S2	URA
pKG313		pFUS1-Ste4-S3tc	pTEF7 Msg5 S47	URA
pKG237		pFUS1-Ste4-S3tc	pTEF7 Msg5 S3	URA
pKG280		pFUS1-Ste4-S3tc	pTEF7 Msg5 ON	URA
pKG228		pFUS1-Ste4-ON	pTEF1-mcherry-CYC1t	URA
pKG311		pFUS1-Ste4-ON	pTEF7 Msg5 OFF	URA

Supplementary Table 3.2. pCS1128-based dual-expression cassette plasmids

pCS #	pKG#	Downstream Cassette	Upstream Cassette	Marker
pCS1128	-	None	pGAL1-yEGFP-CYC1t	TRP
	pKG243	pFUS1-Ste4-OFF	pTEF1-mcherry-CYC1t	TRP
	pKG251	pFUS1-Msg5-OFF	pTEF1-mcherry-CYC1t	TRP
	pKG265	pFUS1-Msg5-OFF	pTEF7 Ste4 S2tc	TRP
	pKG308	pFUS1-Msg5-OFF	pTEF7 Ste4 Stc-OFF1	TRP
	pKG317	pFUS1-Msg5-OFF	pTEF7 Ste4 S3tc	TRP
	pKG267	pFUS1-Msg5-OFF	pTEF7 Ste4 ON	TRP
	pKG248	pFUS1-Msg5-S2	pTEF1-mcherry-CYC1t	TRP
	pKG273	pFUS1-Msg5-S2	pTEF7 Ste4 OFF	TRP
	pKG258	pFUS1-Msg5-S2	pTEF7 Ste4 S2tc	TRP
	pKG299	pFUS1-Msg5-S2	pTEF7 Ste4 Stc-OFF1	TRP
	pKG318	pFUS1-Msg5-S2	pTEF7 Ste4 S3tc	TRP
	pKG260	pFUS1-Msg5-S2	pTEF7 Ste4 ON	TRP
	pKG287	pFUS1-Msg5-S47	pTEF1-mcherry-CYC1t	TRP
	pkG288	pFUS1-Msg5-S47	pTEF7 Ste4 OFF	TRP
	pKG301	pFUS1-Msg5-S47	pTEF7 Ste4 S2tc	TRP
	pKG309	pFUS1-Msg5-S47	pTEF7 Ste4 Stc-OFF1	TRP
	pKG319	pFUS1-Msg5-S47	pTEF7 Ste4 S3tc	TRP
	pKG290	pFUS1-Msg5-S47	pTEF7 Ste4 ON	TRP
	pKG249	pFUS1-Msg5-S3	pTEF1-mcherry-CYC1t	TRP
	pKG291	pFUS1-Msg5-S3	pTEF7 Ste4 OFF	TRP
	pKG268	pFUS1-Msg5-S3	pTEF7 Ste4 S2tc	TRP
	pKG314	pFUS1-Msg5-S3	pTEF7 Ste4 Stc-OFF1	TRP
	pKG320	pFUS1-Msg5-S3	pTEF7 Ste4 S3tc	TRP
	pKG267	pFUS1-Msg5-S3	pTEF7 Ste4 ON	TRP
	pKG250	pFUS1-Msg5-ON	pTEF1-mcherry-CYC1t	TRP
	pKG261	pFUS1-Msg5-ON	pTEF7 Ste4 OFF	TRP
	pKG262	pFUS1-Msg5-ON	pTEF7 Ste4 S2tc	TRP
	pKG315	pFUS1-Msg5-ON	pTEF7 Ste4 Stc-OFF1	TRP

Supplementary Table 3.3. pCS1128-based single-module booster plasmids

pTEF7-Ste4-CYC1t			
pCS #	pKG#	Parent	3'UTR
	pKG321	pCS1128	S4tc
	pKG295	pCS1128	S3tc
	pKG188	pCS1128	S2tc
	pKG182	pCS1128	S1tc
	pKG181	pCS1128	OFF